Leveraging participatory science data to detect and quantify elevational range shifts in birds

Montague H. C. Neate-Clegg*[1,2], Morgan W. Tingley[3], I-Ching Chen[4], Natalia Ocampo-Peñuela[2]

[1]Department of Environmental Science and Policy, University of California Davis, Davis, California, USA

[2]Department of Environmental Studies, University of California Santa Cruz, Santa Cruz, California, USA

[3]Department of Ecology and Evolution, University of California Los Angeles, Los Angeles, California, USA

[4]Department of Life Sciences, National Cheng Kung University, Tainan City, Taiwan

*Corresponding author: mneateclegg@ucdavis.edu

Key words: climate change, citizen science, eBird, elevational gradient, power analysis, range limits, Taiwan

Acknowledgments: we are grateful to all eBird users in Taiwan for contributing their sightings, and to the Cornell Lab of Ornithology for making eBird data freely available.

Abstract

One of the primary expectations—and observed consequences—of persistent warming temperatures is range shifts to higher elevations. However, the ability to detect and attribute climate-driven range shifts has historically been limited to rare locations with sufficient time-series data, which are especially rare outside temperate regions of the Northern Hemisphere. Leveraging data from participatory science programs may offer the key to studying elevational range shifts at broader spatial scales and at higher temporal resolution. With an elevational gradient of almost 4000 m and a high density of checklists from the platform eBird, we focused on the island of Taiwan and demonstrated the estimation of elevational range shifts for 69 species of land bird from 2011–2025. Specifically, we used generalized additive models to estimate species' peak elevations (where occurrence probability is highest), lower and upper elevational limits, and elevational range breadths in every year, and then modeled those estimates over time (while propagating uncertainty) to quantify shift rates. We found that bird species' peak elevations have shifted upslope by 13 m/yr, with lower and upper elevational limits shifting upslope by 8 and 21 m/yr, respectively, leading to range expansions averaging 15 m/yr. We also conducted a power analysis with six hypothetical species to determine the number of presence points necessary to reliably estimate elevational metrics with participatory science data using our methods. We found that, for a single species in a single year, even 100 presences was sufficient to result in 95% coverage of elevational metric estimates 95% of the time. However, accuracy generally decreased for the peak elevations of species that live close to topographic boundaries (sea level or mountaintops). After demonstrating how participatory science data can be used to quantify elevational range shifts, we provide a set of best practices to enable future analyses of elevational ranges and elevational shifts around the world where sufficient eBird data exist.

Introduction

One of the primary expectations of a warming global climate is upslope range shifts (Parmesan & Yohe, 2003; Şekercioğlu et al., 2008), a phenomenon which has now been observed in diverse taxa across the world (I.-C. Chen et al., 2011; Freeman et al., 2021; Lenoir et al., 2020). While mountains serve as direct climate refugia under accelerating warming (de la Fuente et al., 2026), they also face mounting threats such as mountaintop extinctions and extinction debt (Colwell et al., 2008; Freeman, Scholer, et al., 2018). The literature on observed distribution shifts, however, is marked by substantial geographic and taxonomic gaps (Lawlor et al., 2024; Lenoir et al., 2020; Rubenstein et al., 2023), and biological responses to climate change remain highly variable across species and systems (Y.-H. Chen et al., 2025)—all of which pose significant challenges for conservation. While a relative dearth of tropical studies is a commonly cited issue across ecology (Feeley et al., 2017; Harris et al., 2011), studies of elevational shifts are also lacking from subtropical regions, arid regions, and temperate regions in the Southern Hemisphere (Lawlor et al., 2024). Studying elevational redistributions around the world is important not just for filling biogeographical gaps, but for understanding and disentangling the diversity of responses to climate change that can vary from place to place (Freeman et al., 2021; Neate-Clegg et al., 2021; Neate-Clegg & Tingley, 2023).

Empirical studies of elevational range shifts generally require temporally replicated occurrence data across an elevational gradient. Particularly in tropical regions, studies of elevational range shifts have typically relied upon two forms of study design. Perhaps the most common study design is the resurvey, where researchers revisit and sample sites that were originally surveyed decades prior (I.-C. Chen et al., 2009; Forero-Medina et al., 2011; Freeman, Scholer, et al., 2018; Morueta-Holmea et al., 2015; Tingley et al., 2009). However, resurveys rely on the serendipity of the original surveys and also lack the repeated temporal sampling necessary to understand what happens between two time points. The other, less common, form of data come in the form of annual or near-annual standardized surveys

across elevational gradients (Cheng et al., 2019; Neate-Clegg et al., 2018). Such studies have the advantage of allowing researchers to quantify trends over time as well as inter-annual range dynamics (Neate-Clegg, O'Brien, et al., 2020) but they are often much shorter in duration owing to the cost and difficulty of maintaining long-term monitoring programs (Caughlan & Oakley, 2001; Estes et al., 2018). To overcome these limitations, we are in need of a way to fill data gaps in the under-surveyed regions of the world (Goury et al., 2026); to detect and attribute climate-driven range shifts at large spatial scales and fine temporal resolution around the world we cannot rely only on standardized monitoring programs.

Data from participatory science programs could offer a new solution to data shortfalls in under-represented regions. Platforms like eBird (Sullivan et al., 2009) and iNaturalist (www.inaturalist.org) have seen explosive growth in recent years (Mason et al., 2025; Ocampo-Peñuela et al., 2025) and data from these platforms are being used to investigate many aspects of global change ecology, from invasive species (Dimson et al., 2023) to urbanization (Curti et al., 2024) and phenological shifts (Youngflesh et al., 2021). The use of eBird, in particular, has seen a recent significant uptick in tropical countries (Ocampo-Peñuela et al., 2025), and has previously been used along elevational gradients to understand species distributions (Linck, 2025) and patterns of diversity (Freeman et al., 2024), to document altitudinal migration (Somveille et al., 2026; Tsai et al., 2021), and to infer elevational range shifts based on temporal changes in occurrence probability at single sites (Girish & Srinivasan, 2022). eBird has only been globally available since 2010 which has limited the nature of the temporal questions that can be addressed with its data. Yet, after over 15 years and 131 million checklist submissions around the world, we are entering a time when estimating range shifts with eBird data is now possible.

However, participatory science data are not without their pitfalls, and so caution and consideration is needed when using these datasets (Goury et al., 2026; Johnston et al., 2021; Kelling et al., 2019). For one, the participants using the platforms are biased in where they go, often favoring urban greenspaces or high-biodiversity protected areas (Di Cecco et al., 2021; Geurts et al., 2023; Grady et al.,

2026). It is also critical to account for variation in the effort that goes into the observation process (Guillera-Arroita et al., 2015; Kelling et al., 2019; Phillips et al., 2009). eBird does offer advantages over other participatory science programs that can help to minimize these issues (Kelling et al., 2019), including the classification of “complete” checklists—i.e., whether they list all species detected and identified—as well as checklist meta-data including distance and duration, which can be accounted for when modeling distributions (Johnston et al., 2021; Somveille et al., 2026). By leveraging the semi-structured nature of eBird checklists, it is possible to use presence/absence data to model the spatial and temporal patterns of bird occurrence (Callaghan et al., 2025; Neate-Clegg et al., 2023; Youngflesh et al., 2021). Doing so along elevational gradients would allow the widescale characterization of elevational distributions (Freeman et al., 2022) as well as quantification of range dynamics over time (Somveille et al., 2026). For researchers, conservation practitioners, and organizations that want to understand and mitigate the impacts of climate-driven species redistribution but have limited resources for maintaining long-term monitoring programs, eBird could present an invaluable opportunity, especially in areas of high eBird usage (Ocampo-Peñuela et al., 2025).

Taiwan offers an exceptional natural laboratory for studying elevational range shifts with eBird data. Approximately one-third of the island rises over 1000 m above sea level under near-continuous natural vegetation (Y. Y. Chen et al., 2019), up to the highest peak at 3952 m (Yu Shan, 玉山). Taiwan is also home to 157 resident bird species including 32 endemic species and 50 endemic subspecies (Lin et al., 2026; Tsai et al., 2021). Moreover, with over 1.61 million eBird checklists (at the time of writing), Taiwan is ranked 7th in the world in terms of the number of eBird checklists. This is especially impressive as Taiwan’s area is only 36,000 km^2, making it the highest density of checklists (44.7 per km^2) of any eBird subregion (ebird.org/region/world/subregions). The spatiotemporal completeness of Taiwan's eBird data has been improving exponentially over the past decade (Tsai & Tuanmu, 2024), supporting studies of avian altitudinal migration (Tsai et al., 2021) and a comprehensive trait datasets for Taiwan's

avifauna (Fu et al., 2024). This momentum has further culminated in the Taiwan Bird Atlas, a nationwide breeding bird survey launched in 2023 with the goal of completing comprehensive maps of species distribution and abundance by 2028 (TBRI & TWBF, 2023). Taiwan is also suitable for studying climate-driven elevational shifts: long-term observations have shown a sustained and accelerating warming trend, with temperatures rising at 0.15°C per decade over the period 1900–2022, accelerating to 0.27°C per decade since the 1990s (NSTC & MOENV, 2024). Being an island, Taiwan is also less likely to see latitudinal range shifts (Marjakangas et al., 2023), making elevational shifts the most likely spatial response to climate change (Colwell et al., 2008; A. L. Fredston et al., 2025). Finally, straddling the Tropic of Cancer, Taiwan offers a good opportunity to study range shifts in the sub-tropical region.

In this study we provide the first demonstration of how participatory data from eBird can be used to estimate the elevational ranges and shift rates of birds, focusing specifically on 69 species of land bird on the island of Taiwan from 2011 to 2025. We began by using presence/absence data from eBird checklists to model the probability of occurrence across elevation for every species in every year. Specifically, we modeled occurrence using quadratic generalized linear models (GLMs) and generalized additive models (GAMs) while accounting for variation in checklist effort. From these occurrence probability curves we estimated (with associated uncertainty) four elevational metrics for every species in every year: 1) peak occurrence elevation as a measure of central tendency, 2) lower range limit, 3) upper range limit, and 4) elevational range breadth. We then modeled these estimates in Bayesian hierarchical models, while propagating uncertainty, in order to quantify range shifts over time. In addition, to help determine the number of checklists needed to reliably estimate these elevational metrics, we performed a power analysis where we defined six hypothetical species with known elevational positions and used simulated presence/absence data to quantify the coverage and accuracy of metric estimates. Finally, based on our approach, we provide a set of best practices to facilitate future

studies around the world. Our aim is to empower researchers working in different systems to quantify elevational range shifts over ever-increasing timespans and spatial extents.

Methods

Data gathering

We downloaded the eBird Basic Dataset for January 2026, including both the dataset of all checklists and the dataset of all bird records. We used the checklist dataset to define suitable checklists for consideration, applying a series of filters. First, we initially considered checklists from 2010 (the year the eBird platform became globally available) through 2025. We then followed eBird best practices (Johnston et al., 2021), filtering down to "complete" checklists that were "traveling" or "stationary" protocol, ≤ 2 km in distance, 5–300 minutes in duration, and had ≤ 10 observers. Rather than the typical best practice of checklists ≤ 5 km (Johnston et al., 2021), we chose the more stringent distance filter of 2 km (Linck, 2025; Somveille et al., 2026) given how quickly elevation can vary with distance traveled in a topographically complex landscape. From this filtered list of checklists, we extracted unique checklist localities. We then used a digital elevation model (DEM) from USGS (GMTED2010) to extract elevations for each locality, which ranged from -7 to 3878 m asl. We converted elevations below sea level to 0.

Next, we took the full records dataset and filtered down to our selected sites and checklists. Then, for every checklist, we counted the number of species recorded on the list as an additional measure of effort. The reasoning behind this is that, for a given locality and amount of effort, a checklist with twice as many species (often due to higher skill) is more likely to detect a given focal species (Kelling et al., 2015; Szabo et al., 2010), and this number can be included as an effort covariate when modeling eBird data (Boersch-Supan et al., 2019; Horns et al., 2018; Neate-Clegg, Horns, et al., 2020). Given that eBird data span the full annual cycle over which populations are known to vary their elevation with the

seasons (Somveille et al., 2026; Tsai et al., 2021), we chose to focus our study on breeding distributions. We therefore filtered our data to April through August which encompasses the breeding seasons of resident species on the island (Tsai et al., 2021). This step resulted in a dataset of 232,708 checklists across 66,856 sites ranging from sea level to 3878 m (Fig. 1).

We also chose to focus on species not associated with wetland or coastal habitats as such species would be more constrained in their movements (particularly for coastal birds; Somveille et al., 2026). To do this, we aligned the eBird taxonomy with AVONET (Tobias et al., 2022), extracting the primary habitat of each species. We then filtered out species whose primary habitat was “coastal”, “marine”, or “wetland”. In addition, we filtered out species belonging to largely aquatic clades (i.e., Anatidae, Charadriiformes, Pelecaniformes) even if their primary habitat was not water associated. For example, many shorebirds have a primary habitat of “grassland” despite spending most of the annual cycle by water. Finally, we excluded introduced species, which were determined via eBird. We then tabulated the number of records of each species in each year, and considered in our analysis only species:year combinations with ≥ 100 records and species with ≥ 10 unique years of sufficient data, a common threshold for longitudinal studies (McCain et al., 2016; White, 2019). The resulting dataset included 1,470,962 presences of 71 species.

Estimating Annual Elevational Range Metrics

Our analysis consisted of two stages. In the first stage we modeled annual elevational distributions in order to extract key elevational metrics for each species in a given year. In the second stage we modeled change over time in those elevational metrics across all species.

For the first stage, we filtered the datasets down to a single year. We then used the “auk_zerofill” function from the package *auk* to add 0s for every species not present on a given checklist.

This step means that, because we only consider "complete" checklists, every species is either "present" or "absent" on a given checklist. We chose to focus on presence/absence rather than abundance because counts within eBird checklists are relatively scarce and unevenly recorded, while occurrence probability is generally a good proxy for abundance (Gaston et al., 1999; Horns et al., 2018; Walker & Taylor, 2017).

Next, we filtered down to a single species in order to model its occurrence as a function of elevation in a given year. We modeled occurrence in two ways, first in a generalized linear model (GLM) where the effect of elevation is quadratic, and second in a generalized additive model (GAM) with a smooth function on elevation. We chose both approaches in order to compare outputs.

Occurrence for a given species in a given year was modeled in a GLM,

$$Occ_k \sim Bernoulli(p_k)$$

where the presence/absence on checklist *k*, Occ_k, is drawn from a Bernoulli distribution with probability p_k. This probability was then modeled on the logit scale

$$logit(p_k) = \theta_0 + \theta_1 \cdot elev_k + \theta_2 \cdot {elev_k}^2 +$$

$$\theta_3 \cdot distance_k + \theta_4 \cdot duration_k + \theta_5 \cdot n.obs_k + \theta_6 \cdot SR_k$$

as a function of an intercept, θ_0, and six slopes, θ_{1-6}. The slopes $\theta_{1-2,}$ determine the quadratic effect of elevation on occurrence probability while θ_{3-6} are the effort parameters determining the effects of checklist distance (km), duration (minutes), number of observers, and number of species recorded. Number of observers was square-root transformed. For the effort variables, we subtracted 1 from distance, 60 from duration, 1 from number of observers, and 15 from species richness, such that the model intercept reflected the probability of occurrence on a checklist 1 km long, 1 hour in duration, with 1 observer who observed 15 species total. The GAMs had a similar structure but replaced the quadratic

effect of elevation with a smoothing function. Because we wanted to constrain how flexible the smooth function was (e.g., avoiding bimodality), we chose a basis dimension of *k* = 3 which would lead to no more than one peak in occurrence probability (Pedersen et al., 2019).

For every species *i* in every year *j*, we were interested in four key elevational metrics (Fig. 1): 1) peak elevation, $elev_{ij}^{peak}$, i.e., the elevation at which the probability of occurrence was highest; 2) lower limit, $elev_{ij}^{lower}$, i.e., the lowest elevation at which the probability of occurrence was 10% of the maximum probability; 3) upper limit, $elev_{ij}^{upper}$, i.e., the highest elevation at which the probability of occurrence was 10% of the maximum probability; and 4) elevational breadth, $elev_{ij}^{breadth}$, i.e., the elevational range from $elev_{ij}^{upper} - elev_{ij}^{lower}$. We ran a separate GLM and GAM for every species in every year.

Because the occurrence probability curves were estimated with associated uncertainty, it was important for that uncertainty to be captured in the elevational metrics and propagated downstream (A. Fredston, 2024; Linck, 2025). For each model we used a bootstrapping approach where we simulated 1000 sets of coefficients from a multivariate normal distribution based on the model coefficients and variance-covariance matrix. For each simulated set of coefficients, we estimated the four metrics and, across the 1000 simulations, we then calculated the standard deviation of each metric, $\sigma_{elev_{ij}^{m}}$, as a measure of uncertainty (here, *m* is a placeholder for any of the four elevational metrics). The result of this process was point estimates and associated standard deviations for four elevational metrics from a GLM and GAM for every species in every year. We separated these estimates into four datasets, one for every elevational metric.

Many species along elevational gradients have truncated ranges due to topographic boundaries i.e., their elevational ranges end abruptly at sea level or mountaintops. These species present challenges when analyzing range shifts because of elevational metrics estimated at the topographic boundaries. For

example, for a lowland species, its peak elevation in one year may be estimated to be 0 m with a standard deviation ($\sigma_{elev_{ij}^{m}}$) of 0 because the result of every bootstrap simulation was a peak elevation of 0 m. At the other end of the elevational gradient, the same issue is present for metrics estimated to be at the elevation of the highest elevation checklist. Having no uncertainty is statistically and ecologically unrealistic and problematic because we cannot know with total certainty a species' elevational range (A. Fredston, 2024; Linck, 2025). For these reasons, we chose to remove from the peak elevation, lower limit, and upper limit datasets any metrics estimated to be 0 m or at the elevation of the highest elevation checklist. Similarly, for elevational breadth we filtered out breadths estimated to span the entire elevational gradient. As these filtering steps reduced the number of annual estimates for many species, we discarded any species from a particular dataset if it did not have the minimum number of 10 annual estimates in that dataset. Thus, a species occurring close to sea level would be represented in the upper limit and elevational breadth datasets, but not necessarily in the lower limit or peak elevation datasets. Finally, to avoid species whose elevational metrics varied too much from year to year—which could indicate problems in fitting occurrence probability curves—we calculated the standard deviation in estimates across years and removed species from a dataset if the standard deviation in elevational metric was > 500 m. These filtering steps resulted in four datasets of unequal size: 1) a peak elevation dataset of 39 species and 533 species:year combinations; 2) a lower limit dataset of 26 species and 345 species:year combinations; 3) an upper limit dataset of 54 species and 723 species:year combinations; and 4) a range breadth dataset of 68 species and 906 species:year combinations. For each dataset we assessed correlation between the GLM-derived estimates and the GAM-derived estimates.

Modeling Elevational Shifts over Time

In the second stage of the analysis, we modeled changes in elevational metrics over time in Bayesian multi-species hierarchical models, with a separate model for each metric. Our hierarchical models were designed to propagate uncertainty in range estimates from the first step of the analysis, a strength of modeling within a Bayesian framework. Thus, mean elevational metrics (where $m \in \{peak, lower, upper, breadth\}$) were modeled,

$$elev_{ij}^{m} \sim Normal(\mu_{elev_{ij}^{m}}, \sigma_{elev_{ij}^{m}})$$

such that the estimated mean metric of species *i* in year *j* (taken from the previous stage in the analysis) is drawn from a normal distribution with latent true mean $\mu_{elev_{ij}^{m}}$ and estimated standard deviation $\sigma_{elev_{ij}^{m}}$. This step allows the uncertainty in the estimates from the first stage to be propagated throughout the second stage. In turn, this latent mean is drawn from a normal distribution

$$\mu_{elev_{ij}^{m}} \sim Normal(\mu_{Y_{ij}^{m}}, \sigma_{Y^{m}})$$

with species- and year-specific predicted mean $\mu_{Y_{ij}^{m}}$ and standard deviation $\sigma_{Y^{m}}$. The predicted elevational metric is then modeled

$$\mu_{Y_{ij}^{m}} = \alpha_{i}^{m} + \beta_{i}^{m} \cdot year_{j}$$

as a function of species-specific intercepts, α_{i}^{m}, and linear effect of year, β_{i}^{m}. In order to produce more accurate species-specific estimates that avoided model shrinkage, we treated species as fixed effects, with each species-specific parameter being drawn from vague priors. We then derived within the model the overall shift rate across species, μ_{β}^{m}, as the mean of all β_{i}^{m}. For each model, we used vague priors and we ran the model for 100,000 iterations over three chains with a burn-in of 10,000 and 90-fold thinning, resulting in 3000 posteriors. We attributed model convergence when all rhats were ≤ 1.01.

From each model we extracted the mean μ_β^m and β_i^m parameter values and associated 95% Bayesian credible intervals. We considered shift rates to have "strong evidence" when ($\Pr(|\mu_\beta^m| > 0) > 95\%$).

Having compared the GLM-derived estimates and the GAM-derived estimates from the first stage, we chose to focus on the estimates from the GAMs because they a) did not impose symmetrical peaks in occurrence across elevation (Burner et al., 2019; Freeman & Beehler, 2018; Linck, 2025) and b) allowed for plateaus in occurrence probability at topographic limits—i.e., sea level or mountaintops. We therefore report principally on shift rates based on models of the GAM-derived estimates. However, we also conducted a sensitivity analysis using the GLM-derived estimates (see below).

Sensitivity Analyses

In addition to our models of ranges based on GAM-derived elevational metrics, we also performed the same models on our GLM-derived estimates from the first stage, comparing the overall (μ_β^m) and species-specific shift rates (β_i^m). We also compared our main results to models based on GAM-derived elevational metrics where the uncertainty in those metrics was not propagated in the model.

As a further counterpoint, we considered simpler elevational metrics that were not derived from elevation-based occurrence probability curves. These simple metrics were chosen based on their common use in other studies of elevational ranges (Brodie et al., 2025; Linck, 2025; Neate-Clegg, O'Brien, et al., 2020; Rubenstein et al., 2023; Tsai et al., 2021). Specifically, for every species in every year we took the elevations of all presences and calculated 1) the mean as a proxy for peak elevation, 2) the 2.5th percentile as a proxy for lower limit, 3) the 97.5th percentile as a proxy for the upper limit, and 4) the 95th inter-percentile range (97.5th percentile – 2.5th percentile) as a proxy for elevational breadth. We

conducted the same models as above (without error propagation) and compared the shift rate estimates to our main results.

Power Analyses

In order to estimate elevational metrics and, from these, elevational shift rates, a pertinent question is: how many checklists or presence points does one need? We therefore undertook a power analysis to answer this question (Johnson et al., 2015). In this power analysis we ran models as above on simulated data where we knew the true underlying elevational metrics, and assessed how close estimated metrics were to the "truth".

We began by creating six species with pre-defined occurrence probability curves. Species A was defined to be a common (highest occurrence probability around 0.9) mid-elevation species with a peak elevation of 1600 m, trailing off to clear upper and lower range limits. Species B was a common lowland species with a peak elevation of 100 m, and species C was a common highland species with a peak elevation of 3500 m. To these species we added species D, E, and F, which shared the same peak elevations as A–C but were much less common (highest occurrence probabilities around 0.1). Next, we took all the checklists that followed best practices from all months, 2011–2025, filtering out checklists above 3600 m to create a hard upper bound. These 593,410 checklists represent the uneven spatial effort in eBird activity across elevations, highly skewed toward the lowlands (Fig. S1), which is to be expected in most systems. For the simulation process, the checklist locations defined where the simulated observation process took place and the occurrence probability curves defined the true probability of observing the focal species. We also defined a list of sample sizes, *n*, for the number of presence points to test in the power analysis, ranging from n = 75 to n = 5000.

In every simulation, we began by randomly drawing a 1 or 0 for every single checklist from a Bernoulli trial with a probability equal to the predicted probability of occurrence for the focal species at that elevation. From this simulated dataset, we calculated the proportion of presences, *P*, and then randomly drew without replacement a subset of *n* presences. Because we wanted the subset of presences and absences to be proportional to the full set, we also randomly drew $n * \frac{1-P}{P}$ absences and combined them with the subset of presences. For example, when *P* = 0.25, a random subset of 100 presences would be combined with a random subset of 300 random.

To the subset of simulated data, we next applied quadratic GLMs as above (given the symmetry we imposed on the distributions), bootstrapping the model coefficients and extracting the same four elevational metrics and associated uncertainty. To assess the coverage of an estimate, we determined whether the 95% confidence interval of the estimate included the "true" elevational metric. To assess the accuracy of an estimate, we determined the difference between the estimate and the true elevational metric, which we then binarized to determine whether the estimate was 1) within 50 m of the true metric, 2) within 25 m, and 3) within 10 m. For every value of *n*, we performed 100 simulations and then calculated the percentage of simulations that resulted in positive outcomes (either overlapping confidence intervals or estimates within the threshold distance). Finally, we plotted how these percentages varied as a function of *n*. We considered a sample size to have suitable power above the typical threshold of 80%.

Results

Range Shifts

Overall, we were able to analyze range shifts across 69 species, although the number of species varied depending on the elevational metric considered. For the 39 species whose peak occurrence elevations occurred away from topographic boundaries (Fig. 3a), we found strong evidence that peak elevations shifted upslope at a rate of 13.2 m/yr (Bayesian credible interval [CrI]: 11.8 to 14.6 m/yr; Pr[$\mu_{\beta}^{peak} > 0$] = 100%). Species-specific shift rates (Fig. 4a) ranged from -0.3 m/yr (*Liocichla steerii*; CrI: -7.0 to 6.4) to 32.0 m/yr (*Alcippe morrisonia*; CrI: 25.0 to 38.9), with strong evidence of upslope shifts for 31 species (79%). For no species was there strong evidence of downslope shifts.

Shifts in peak elevation could result from shifts at either range limit. For the 26 species whose lower limits generally occurred above sea level (Fig. 3b), there was strong evidence that lower limits shifted up slope at a rate of 8.0 m/yr (CrI: 5.9 to 10.1 m/yr; Pr[$\mu_{\beta}^{lower} > 0$] = 100%). Species-specific shift rates (Fig. 4b) ranged from -8.4 m/yr (*Trochalopteron morrisonianum*; CrI: -18.0 to 1.3) to 26.8 m/yr (*Spizixos semitorques*; CrI: 14.8 to 39.0), with strong evidence of upslope shifts for 11 species (42%). By comparison, for the 54 species whose upper limits generally occurred below the mountaintops (Fig. 3c), there was strong evidence that upper limits shifted up slope at a rate of 20.8 m/yr (CrI: 17.5 to 24.1 m/yr; Pr[$\mu_{\beta}^{upper} > 0$] = 100%). Species-specific shift rates (Fig. 4c) ranged from -7.9 m/yr (*Cyanoderma ruficeps*; CrI: -25.4 to 9.7) to 67.8 m/yr (*Passer montanus*; CrI: 49.0 to 86.5), with strong evidence of upslope shifts for 18 species (33%). With upper limits shifting faster than lower limits, there was strong evidence across 68 species (Fig. 3d) that elevational range breadths expanded at a rate of 14.9/yr (CrI: 11.7 to 17.9 m/yr; Pr[$\mu_{\beta}^{rng} > 0$] = 100%). Species-specific changes (Fig. 4d) ranged from -20.6 m/yr (*Horornis fortipes*; CrI: -44.7 to 3.0) to 69.4 m/yr (*P. montanus*; CrI: 47.8 to 90.7), with strong evidence of range expansions for 17 species (25%).

Sensitivity Analysis

GLM-derived estimates of peak elevation were highly correlated (Fig. S2) with GAM-derived estimates ($r \approx 1$) and fell along the 1:1 line, and the same was true for lower limits ($r \approx 1$), upper limits ($r \approx 1$), and range breadths ($r = 0.99$). The resulting GLM-derived models produced very similar overall shift rate estimates to the GAM-derived results, with peak elevation shifting by 11.5 m/yr (CrI: 10.0 to 13.1 m/yr; $\Pr[\mu_{\beta}^{peak} > 0] = 100\%$), lower limits by 6.8 m/yr (CrI: 4.8 to 8.8 m/yr; $\Pr[\mu_{\beta}^{lower} > 0] = 100\%$), upper limits by 20.6 m/yr (CrI: 17.4 to 23.7 m/yr; $\Pr[\mu_{\beta}^{upper} > 0] = 100\%$), and elevational range breadths expanding by 15.6 m/yr (CrI: 12.5 to 18.5 m/yr; $\Pr[\mu_{\beta}^{breadth} > 0] = 100\%$). The species-specific shift rates were also highly correlated with those from the GAM-derived estimates (Fig. S3) for: peak elevations $r = 0.90$, lower limits $r = 0.98$, upper limits $r = 0.96$, elevational breadths $r = 0.96$. GLM- and GAM-derived shift rates generally fell along the 1:1 line but for peak elevation and lower limit shift rates which were estimated to be slightly higher based on GAM-derived estimates. These sensitivity analyses suggest similar shift rate results after modeling occurrence probability with either a GAM or GLM.

In models where uncertainty from the first stage was not propagated, the overall shift rates were fairly similar to the main results. Peak elevations shifted by 13.7 m/yr (CrI: 12.0 to 15.6 m/yr; $\Pr[\mu_{\beta}^{peak} > 0] = 100\%$), lower limits by 6.9 m/yr (CrI: 4.7 to 9.2 m/yr; $\Pr[\mu_{\beta}^{lower} > 0] = 100\%$), upper limits by 20.9 m/yr (CrI: 17.5 to 24.3 m/yr; $\Pr[\mu_{\beta}^{upper} > 0] = 100\%$), and elevational breadths expanded by 15.7 m/yr (CrI: 12.2 to 19.0 m/yr; $\Pr[\mu_{\beta}^{breadth} > 0] = 100\%$). Correlation among species-specific shift rates (Fig. S4) was high for lower limits ($r = 0.96$), upper limits ($r = 0.98$), and elevational breadths ($r = 0.98$), but was not high for peak elevations ($r = 0.62$). Shift-rate estimates also tended to fall along the 1:1 line. These

sensitivity analyses suggest that error propagation is preferable when estimating species-specific shift rates in peak elevation.

When considering simple elevational metrics that were not derived from elevation-based occurrence probability curves, correlation was generally high (Fig. S5) between peak elevations and the mean elevation of presences (r = 0.97), between lower limits and the 2.5th percentile of presences (r = 0.95), between upper limits and the 97.5th percentile of presences (r = 0.95), and between elevational breadths and the 90th inter-percentile range (r = 0.90). However, for peak elevations, upper limits, and elevational breadth, these metrics were biased much lower in elevation than the GAM-derived estimates, likely owing to the high density of checklists at lower elevations. The downstream models based on these metrics produced overall shift rate estimates that differed markedly from our main results. Mean elevation of presences was predicted to have shifted by -0.6 m/yr (CrI: -2.5 to 1.4 m/yr; $\Pr[\mu_{\beta}^{peak} < 0] = 72\%$); 2.5th percentiles of presences were predicted to have shifted by -4.5 m/yr (CrI: -8.9 to -0.1 m/yr; $\Pr[\mu_{\beta}^{lower} < 0] = 98\%$); 97.5th percentiles of presences were predicted to have shifted by 7.5 m/yr (CrI: 4.8 to 10.4 m/yr; $\Pr[\mu_{\beta}^{upper} > 0] \approx 100\%$), and 95th inter-percentile range was predicted to have expanded by 7.9 m/yr (CrI: 4.9 to 10.9 m/yr; $\Pr[\mu_{\beta}^{breadth} > 0] = 100\%$). Correlation among species-specific shift rates was low (Fig. S6) for peak elevations (r = 0.23), lower limits (r = 0.55), upper limits (r = 0.21), elevational breadths (r = -0.04). These sensitivity analyses show that using simple elevational metrics based only on presences is not suitable for estimating elevational shift rates.

Power Analysis

For the six hypothetical species (Fig. 5), we found that coverage—i.e., the percentage of times that the 95% confidence interval of an estimate overlapped the “true” metric value—was generally very high

(above 95%) across values of *n* (number of presence points). Thus, the uncertainty around each estimate tended to include the true value.

In contrast, there was much more variation in accuracy depending on *n* and the commonness or elevational position of the hypothetical species. For species A (common mid-elevation species), accuracy within 50 m of the truth was achieved with 100 presences for peak elevation and lower limit, and 200 presences for upper limit. To be within 10 m of the truth, the threshold was much higher: ranging from 2000 presences for peak elevation to 5000 presences for upper limit. A similar pattern was evident for species D (scarce mid-elevation species) but with 200 or 300 presences needed for 50 m accuracy for the lower and upper limits, respectively. For species B (common lowland species) accuracy was generally much lower than for species A, requiring over 5000 presences for the upper limit to be within 50 m, and accuracy was even lower for peak elevation. In species E (scarce lowland species) accuracy was actually higher for peak elevation—requiring 4500 presences for accuracy within 50 m—than for upper limit. For species C (common highland species), accuracy was generally high for the lower limit, requiring only 200 presences to be within 50 m, and 1000 presences to be within 25 m, but accuracy was much lower for peak elevation. Finally, for species F (scarce highland species), patterns mirrored species C but with lower accuracy overall.

Discussion

In an era of climate-driven species redistribution (Lenoir et al., 2020), detecting and quantifying elevational range shifts at increasing spatial, temporal, and taxonomic scales is critical but has been historically limited to resurveys, long-term monitoring programs, and opportunistic data which themselves are geographically biased (Feeley et al., 2017). Participatory science data could offer the key to upscaling the analysis of elevational range dynamics (Somveille et al., 2026; Tsai et al., 2021). Here, we

demonstrate for the first time the use of occurrence data from eBird to quantify elevational range shifts, finding upslope range shifts and elevational range expansions across 69 species of land bird in Taiwan (Fig. 3). Specifically, we found that species shifted their peak elevations by 13 m/yr, their lower limits by 8 m/yr, and their upper limits by 21 m/yr, resulting in range expansions of 15 m/yr. Although these results are based on slightly different pools of species—e.g., lower limits for highland species, upper limits for lowland species—the rate of range expansion is almost exactly intermediate between the shift rates of lower and upper limits, and overlaps the peak elevation shift rate. There was also notable consistency in shift rates across species (Fig. 4). While, many studies have found high heterogeneity in shift rates including a substantial proportion of species that have shifted downslope (Neate-Clegg et al., 2021; Rumpf et al., 2019; Tingley et al., 2012), we found positive shift rates in peak elevations for 97% of species, in lower limits for 77% of species, and in upper limits for 94% of species.

The consistency of upslope shifts could be indicative of Taiwan's natural land cover. Approximately 65% of the island is forested with very little deforestation above 100 m (Y. Y. Chen et al., 2019), and this continuity in forest cover could allow species to shift at a relatively fast rate. The finding that upper limits have shifted faster than lower limits is consistent with another study of Asian birds in New Guinea (Freeman & Class Freeman, 2014) but this pattern is far from universal with meta-analyses varying in whether they found faster shift rates in species' lower or upper limits (Freeman, Lee-Yaw, et al., 2018; Neate-Clegg et al., 2021; Rumpf et al., 2019). One possible explanation is that many lowland birds are urban associated and their ranges may be expanding with increased human development at higher elevations (Y. Y. Chen et al., 2019; Greig et al., 2017). For example, the species that shifted its upper limits the fastest, Eurasian Tree Sparrow (*Passer montanus*), is very abundant in urban and suburban habitats and has seen increases in mid-elevation towns (Wu et al., 2012). That species' lower limits are not shifting as rapidly could also be due to the preservation of habitats at lower elevation in Taiwan. Many parts of the world have seen high levels of deforestation in the lowlands (Namkhan et al.,

2021) and this is expected to cause species lower limits to contract upslope (Harris et al., 2014; Ocampo-Peñuela & Pimm, 2015). Given that lower (warmer) range limits are also thought to be more limited by biotic interactions than abiotic factors (Darwin, 1859; Louthan et al., 2015; Paquette & Hargreaves, 2021), the slower shift rates could indicate a lack of natural enemies or competitors (Alexander et al., 2015; Matysioková & Remeš, 2022; Paxton et al., 2016; Tsai et al., 2021).

Detecting elevational range shifts is particularly important for species of conservation concern such as range-restricted species or threatened species. Of the 32 endemic birds of Taiwan, 20 had sufficient data to be represented in our study (Fig. 4). Of these there was strong evidence of upslope shifts in the peak elevations of 10 out of 14 species, the lower limits of 2 out of 14 species, and the upper limits of 3 out of 12 species. This resulted in range expansions for 4 out of the 20 species. Our datasets also included one species listed as vulnerable by the IUCN (Birdlife International, 2025), the endemic Styan's Bulbul (*Pycnonotus taivanus*), which did not show strong evidence of upslope shifts. Although evidence of range contractions in these species was low, concern should be paid to highland species whose lower limits are shifting upslope, including the endemic Taiwan Bush Warbler (*Locustella alishanensis*) and Taiwan Yuhina (*Yuhina brunneiceps*). Moreover, there are endemic species, including the near threatened Swinhoe's Pheasant (*Lophura swinhoii*) and Taiwan Rosefinch (*Carpodacus formosanus*), for which we lacked sufficient data to include them in the analyses but that could be experiencing range contractions. Of particular note is *Prunella collaris fennelli*, an endemic subspecies of Alpine Accentor which lives in open habitat on only the highest peaks in Taiwan (Wu et al., 2012), where tree line has expanded upslope (Greenwood et al., 2014) and precipitation has become more variable (Kuo et al., 2022). In years to come, more checklists may allow us to model the ranges and range shifts of these scarcer species, and the resulting observations could be incorporated into threat assessments for Taiwan's endemic birds.

Being able to quantify elevational shift rates is critical to the conservation of species along elevational gradients. For mountaintop species it is important to know whether their ranges are contracting as a precursor to extirpation or extinction (Freeman, Scholer, et al., 2018). For regions where species are shifting quickly, prioritizing protected areas or restoring habitat along continuous gradients should be a priority (Elsen et al., 2018; Lawler et al., 2015). And for species that aren't shifting, we need to know whether remaining in place is maladaptive or not (A. L. Fredston et al., 2025; Neate-Clegg et al., 2024). Modeling shift rates themselves requires being able to reliably estimate elevational range metrics in a given time point. Doing so can be relatively straightforward when data come from standardized survey effort across elevational gradients, but the availability of such datasets is relatively rare and geographically biased (Lawlor et al., 2024), due in large part to the funds and logistics needed to maintain long-term monitoring programs (Caughlan & Oakley, 2001). Participatory science data could unlock the potential for researches to quantify elevational distributions and range shifts in an increasing number of mountain ranges (Somveille et al., 2026), filling biogeographical gaps and democratizing the ability to determine spatiotemporal variation in elevational ranges and evaluate local climate change responses (Theobald et al., 2015). Moreover, using standardized approaches could facilitate comparisons both at different time points and among locations, aiding meta-analytical studies (Lawlor et al., 2024; Linck, 2025).

However, participatory science data present challenges due to biases in effort (Geurts et al., 2023; Kelling et al., 2019). In particular, where people submit eBird checklists is often spatially biased including along elevational gradients (Fig. S1). Taking the mean elevation of all presences would therefore be biased toward where people spend most time birding i.e., lowlands. Indeed, we found that simple metrics based only on presence data (e.g., mean elevation, 95% percentiles) were biased toward lower elevations (Fig. S5) and resulted in range shift estimates vastly different from our main results (Fig. S6). A way to circumvent this issue would be to spatially rarefy the checklists to have equal

representation at each elevational band, but this would involve discarding the vast majority of checklists. Instead, one of the great advantages of eBird is the existence of "complete checklists" which allows us to distinguish presences from absences without having to generate pseudo-absences, and to model those presence/absences as a function of spatial covariates like elevation (Johnston et al., 2021). Moreover, eBird checklists also vary in distance, duration, and number of observers, which can create bias when birdwatchers put more effort in within nicer habitat, but these effort covariates can also be accounted for in the models to reduce the effects of effort bias (Boersch-Supan et al., 2019; Horns et al., 2018; Johnston et al., 2021; Neate-Clegg, Horns, et al., 2020). Thus, occurrence probability curves can be fit with presence/absence data that account for variation in effort.

Whether to model occurrence probability with a GAM or quadratic GLM resulted in very similar estimates of elevational metrics and shift rates (Figs. S1, S2). However, the GAM approach is likely more suitable because it removes the assumption that species have symmetrical hump-shaped distributions (Burner et al., 2019; Freeman & Beehler, 2018; Linck, 2025). In addition to the variation in the observation process, there is also statistical uncertainty when estimating species' elevational ranges (A. Fredston, 2024; Linck, 2025). Although occurrence models effectively control for variation in the number of checklists, uncertainty in occurrence probability can be much higher when there are fewer data points i.e., at higher elevations (e.g., Fig. 2c). When modeling estimates of range position it is therefore critical to not treat those data points as known with certainty, but to propagate the uncertainty downstream (Gilbert et al., 2023; Jenouvrier, 2013; Linck, 2025). Although we generally found high correlation between range limit shift rates with and without error propagation, this may not be generalizable to locations with lower sample sizes and higher uncertainty. For example, in our power analyses, we showed that the accuracy of elevational metric estimates is often quite low (Fig. 5), especially below 1000 presence points. However, we did find that, for almost all situations, the 95% confidence intervals of estimates overlapped the true values. These results support the use of error propagation when

modeling elevational range shifts. By explicitly incorporating the uncertainty in our estimates of elevational metrics we are allowing for the possibility that the true value that we cannot know is somewhere within the range of our estimate.

The power analyses also revealed important general patterns across species and elevational metrics. First, accuracy of estimates was generally higher for mid-elevation species, whether they were common or scarce. This finding means that if a species' whole elevational range is contained within an elevational gradient (i.e., doesn't reach either topographic limit), with 100-200 presences its peak elevation and range limits can be estimated with good coverage and accuracy within 50 m. For lowland species, accuracy was generally lower and this is likely due to the true peak elevation being close to, but not actually at a topographic limit (sea level). The peak elevation itself is hard to estimate as many occurrence probability curves end up being concave (rather than the hump-shaped curves in Fig. 2) with the highest probability of occurrence at sea level. However, accuracy was generally higher for the upper limit which occurs much farther from a topographic boundary. For similar reasons, the lower limits of highland species could be estimated with relatively high accuracy based on 200-600 presences, while the accuracy was much lower for their peak elevations. Interestingly, the accuracy of peak elevation estimates was roughly similar for lowland and highland species alike, whether they were common or scarce, suggesting that the total number of presences mattered more than the relative proportion of absences (Liu et al., 2019). However, lower limits for highland species had much higher accuracy than upper limits for lowland species, perhaps due to greater amount of land and higher habitat heterogeneity at lower elevations (Y. Y. Chen et al., 2019).

We have demonstrated an analytical framework and power analysis to use participatory science data to detect and quantify elevational range shifts. Having shown its utility with the Taiwan case study, we make the following recommendations to those wishing to apply this framework in other mountain ranges:

1. Rather than taking simple metrics such as the mean elevation of occurrences, model occurrence probability as a function of elevation.
2. Include effort variables as covariates when modeling occurrence probability.
3. Use a GAM including a smooth function on elevation with a basis dimension of 3 (i.e., $k = 3$) in order to estimate an occurrence probability curve with a single maximum but without the constraint of symmetry.
4. Record uncertainty in estimates of elevational metrics and propagate that uncertainty when modeling range shifts.
5. Estimate peak elevations and both range limits for species whose ranges fall entirely within topographic boundaries, but for lowland species focus on upper limits and for highland species focus on lower limits.
6. For 95% confidence intervals with suitable coverage, model occurrence probabilities for species with a minimum of 100 presences, ideally 200-500. Ignoring uncertainty would require much larger sample sizes.

While these guidelines are intended for estimating elevational metrics from presence/absence data, many of these principles would also apply to modeling occurrence across other spatial gradients (e.g., latitude or urbanization). They may also apply to presence-only participatory science data for other taxa, such as from iNaturalist or GBIF. However, with presence-only data, additional caution is needed because biases in where people observe wildlife can lead to biases in the factors that predict their occurrence (Guillera-Arroita et al., 2015; Kelling et al., 2019; Phillips et al., 2009). Besides these recommendations for estimating elevational metrics, we follow other studies in recommending a minimum of 10 years of estimates when modeling temporal trends (McCain et al., 2016; White, 2019).

In this study, we were able to estimate elevational metrics over ten years for 69 species, with 2011 being the earliest year with sufficient data (100 presences) for the most common species. This feat

is contextualized by the fact that Taiwan has the highest density of checklists (45 checklists per km^2) in the top 20 world subregions (https://ebird.org/region/world/subregions), with the next highest densities being in Costa Rica (27 checklists per km^2) and the UK (11 checklists per km^2), followed by the US (8 checklists per km^2). We therefore do not expect many countries to yet have the temporal and spatial resolution to estimate elevational metrics for dozens of species over a ten-year period. However, what matters is not the per-country density, but the density of checklists over elevational gradients. As the use of eBird continues to increase, especially in tropical countries (Ocampo-Peñuela et al., 2025), we can be hopeful that elevational gradients with heavy birdwatching activity—such as the Manu Road in Peru or the Sierra Nevada de Santa Marta in Colombia—will soon reach this threshold. As such locations reach data sufficiency, we hope to see the characterization of elevational ranges and analysis of range shifts for an increasing number of species in an increasing number of locations.

References

Alexander, J. M., Diez, J. M., & Levine, J. M. (2015). Novel competitors shape species' responses to climate change. *Nature*, *525*(7570), 515–518. https://doi.org/10.1038/nature14952

Birdlife International. (2025). *BirdLife Data Zone*. http://datazone.birdlife.org/species

Boersch-Supan, P. H., Trask, A. E., & Baillie, S. R. (2019). Robustness of simple avian population trend models for semi-structured citizen science data is species-dependent. *Biological Conservation*, *240*. https://doi.org/10.1016/j.biocon.2019.108286

Brodie, J. F., Freeman, B. G., Mannion, P. D., & Hargreaves, A. L. (2025). Shifting, expanding, or contracting? Range movement consequences for biodiversity. *Trends in Ecology and Evolution*, *40*(5), 439–448. https://doi.org/10.1016/j.tree.2025.02.001

Burner, R. C., Styring, A. R., Rahman, M. A., & Sheldon, F. H. (2019). Occupancy patterns and upper range limits of lowland Bornean birds along an elevational gradient. *Journal of Biogeography*, *46*(11), 2583–2596. https://doi.org/10.1111/jbi.13691

Callaghan, C. T., Venegas-Li, R., Mason, B. M., Fuller, R. A., Spake, R., & Watson, J. E. M. (2025). High-Integrity Forests Are Critical for Forest Specialist Birds. *Global Ecology and Biogeography*, *34*(9). https://doi.org/10.1111/geb.70118

Caughlan, L., & Oakley, K. L. (2001). Cost considerations for long-term ecological monitoring. *Ecological Indicators*, *1*(2), 123–134. https://doi.org/10.1016/s1470-160x(01)00015-2

Chen, I.-C., Hill, J. K., Ohlemüller, R., Roy, D. B., & Thomas, C. D. (2011). Rapid range shifts of species associated with high levels of climate change. *Science*, *333*, 1024–1026.

Chen, I.-C., Shiu, H.-J., Benedick, S., Holloway, J. D., Chey, V. K., Barlow, H. S., Hill, J. K., & Thomas, C. D.

(2009). Elevation increases in moth assemblages over 42 years on a tropical mountain. *Proceedings of the National Academy of Sciences*, *106*(5), 1479–1483. https://doi.org/10.1073/pnas.0809320106

Chen, Y.-H., Lenoir, J., & Chen, C. (2025). *Limited evidence for range shift – driven extinction in mountain biota*. *May*, 741–747. https://doi.org/10.1126/science.adq9512

Chen, Y. Y., Huang, W., Wang, W. H., Juang, J. Y., Hong, J. S., Kato, T., & Luyssaert, S. (2019). Reconstructing Taiwan's land cover changes between 1904 and 2015 from historical maps and satellite images. *Scientific Reports*, *9*(1), 1–12. https://doi.org/10.1038/s41598-019-40063-1

Cheng, W., Kendrick, R. C., Guo, F., Xing, S., Tingley, M. W., & Bonebrake, T. C. (2019). Complex elevational shifts in a tropical lowland moth community following a decade of climate change. *Diversity and Distributions*, *25*(4), 514–523. https://doi.org/10.1111/ddi.12864

Colwell, R. K., Brehm, G., Cardelús, C. L., Gilman, A. C., & Longino, J. T. (2008). Global warming, elevational range shifts, and lowland biotic attrition in the Wet Tropics. *Science*, *322*(October), 258–261. https://doi.org/10.1126/science.1162547

Curti, J. N., Barton, M., Flores, R. G., Lechner, M., Lipman, A., Montgomery, G. A., Park, A. Y., Rochel, K., & Tingley, M. W. (2024). Using unstructured crowd-sourced data to evaluate urban tolerance of terrestrial native animal species within a California Mega-City. *PLoS ONE*, *19*(5 May), 1–21. https://doi.org/10.1371/journal.pone.0295476

Darwin, C. (1859). *On the Origin of Species by Means of Natural Selection, Or The Preservation of Favoured Races in the Struggle for Life*. John Murray.

de la Fuente, A., Chen, I. C., Briscoe, N. J., & Kearney, M. R. (2026). Mountains magnify mechanisms in climate change biology. In *Nature Climate Change* (Vol. 16, Issue 2, pp. 115–117).

https://doi.org/10.1038/s41558-025-02549-x

Di Cecco, G. J., Barve, V., Belitz, M. W., Stucky, B. J., Guralnick, R. P., & Hurlbert, A. H. (2021). Observing the Observers: How Participants Contribute Data to iNaturalist and Implications for Biodiversity Science. *BioScience*, *71*(11), 1179–1188. https://doi.org/10.1093/biosci/biab093

Dimson, M., Berio Fortini, L., Tingley, M. W., & Gillespie, T. W. (2023). Citizen science can complement professional invasive plant surveys and improve estimates of suitable habitat. *Diversity and Distributions*, *29*(9), 1141–1156. https://doi.org/10.1111/DDI.13749

Elsen, P. R., Monahan, W. B., & Merenlender, A. M. (2018). Global patterns of protection of elevational gradients in mountain ranges. *Proceedings of the National Academy of Sciences*, *115*(23), 6004–6009. https://doi.org/10.1073/pnas.1720141115

Estes, L., Elsen, P. R., Treuer, T., Ahmed, L., Caylor, K., Chang, J., Choi, J. J., & Ellis, E. C. (2018). The spatial and temporal domains of modern ecology. *Nature Ecology & Evolution*, *2*(May). https://doi.org/10.1038/s41559-018-0524-4

Feeley, K. J., Stroud, J. T., & Perez, T. M. (2017). Most 'global' reviews of species' responses to climate change are not truly global. *Diversity and Distributions*, *23*(3), 231–234. https://doi.org/10.1111/ddi.12517

Forero-Medina, G., Terborgh, J., Socolar, S. J., & Pimm, S. L. (2011). Elevational ranges of birds on a tropical montane gradient lag behind warming temperatures. *PLoS ONE*, *6*(12), e28535. https://doi.org/10.1371/journal.pone.0028535

Fredston, A. (2024). Measuring the edges of species' geographic ranges. *EcoEvoRxiv*.

Fredston, A. L., Tingley, M. W., Neate-Clegg, M. H. C., Evans, L. J., Antão, L. H., Ban, N. C., Chen, I., Chen, Y., Comte, L., Edwards, D. P., Evengard, B., Fadrique, B., Falkeis, S. H., Guralnick, R., Pauchard, A.,

Pecl, G., Pinsky, M. L., Senior, R. A., Smith, J. E., … Scheffers, B. R. (2025). Reimagining species on the move across space and time. *Trends in Ecology & Evolution*, *xx*(xx), 1–10. https://doi.org/10.1016/j.tree.2025.03.015

Freeman, B. G., & Beehler, B. M. (2018). Limited support for the "abundant centre" hypothesis in birds along a tropical elevational gradient: implications for the fate of lowland tropical species in a warmer future. *Journal of Biogeography*, *45*(8), 1884–1895. https://doi.org/10.1111/jbi.13370

Freeman, B. G., & Class Freeman, A. M. (2014). Rapid upslope shifts in New Guinean birds illustrate strong distributional responses of tropical montane species to global warming. *Proceedings of the National Academy of Sciences*, *111*(12), 4490–4494. https://doi.org/10.1073/pnas.1318190111

Freeman, B. G., Lee-Yaw, J. A., Sunday, J. M., & Hargreaves, A. L. (2018). Expanding, shifting and shrinking: The impact of global warming on species' elevational distributions. *Global Ecology and Biogeography*, *27*(11), 1268–1276. https://doi.org/10.1111/geb.12774

Freeman, B. G., Miller, E. T., & Strimas-Mackey, M. (2024). Interspecific competition shapes bird species' distributions along tropical precipitation gradients. *Ecology Letters*, *27*(8), e14487. https://doi.org/10.1111/ELE.14487;ISSUE:ISSUE:DOI

Freeman, B. G., Scholer, M. N., Ruiz-Gutierrez, V., & Fitzpatrick, J. W. (2018). Climate change causes upslope shifts and mountaintop extirpations in a tropical bird community. *Proceedings of the National Academy of Sciences*, *115*(47), 11982–11987. https://doi.org/10.1073/pnas.1804224115

Freeman, B. G., Song, Y., Feeley, K. J., & Zhu, K. (2021). Montane species track rising temperatures better in the tropics than in the temperate zone. *Ecology Letters*. https://doi.org/10.1111/ele.13762

Freeman, B. G., Strimas-Mackey, M., & Miller, E. T. (2022). Interspecific competition limits bird species' ranges in tropical mountains. *Science*, *377*(6604), 416–420.

https://doi.org/10.1126/SCIENCE.ABL7242

Fu, S.-W., Feng, M.-C., Chi, P.-W., & Ding, T.-S. (2024). Combining citizen science data and literature to build a traits dataset of Taiwan ' s birds. *Scientific Data*, 1–8. https://doi.org/10.1038/s41597-024-03928-3

Gaston, K. J., Blackburn, T. I. M. M., & Gregory, R. D. (1999). *Intraspecific abundance – occupancy relationships : case studies of six bird species in Britain*. 197–212.

Geurts, E. M., Reynolds, J. D., & Starzomski, B. M. (2023). Turning observations into biodiversity data: Broadscale spatial biases in community science. *Ecosphere*, *14*(6), 1–13. https://doi.org/10.1002/ecs2.4582

Gilbert, N. A., Eyster, H. N., & Zipkin, E. F. (2023). Propagating uncertainty in ecological models to understand causation. *Frontiers in Ecology and the Environment*, *21*(3), 114–115. https://doi.org/10.1002/fee.2610

Girish, K. S., & Srinivasan, U. (2022). Community science data provide evidence for upward elevational range shifts by Eastern Himalayan birds. *Biotropica*. https://doi.org/10.1111/btp.13133

Goury, R., Bowler, D. E., Harrower, C., Münkemüller, T., Vallet, J., Yearsley, J. M., Thuiller, W., & Pescott, O. L. (2026). *A practical guide to species trend detection with unstructured data using local frequency scaling (Frescalo)*. 1–14. https://doi.org/10.1002/ecog.08270

Grady, E. L., Campbell, C. J., Callaghan, C. T., & Guralnick, R. P. (2026). iNaturalist Users Exhibit Distinct Spatiotemporal Sampling Preferences, with Implications for Biodiversity Science and Project Planning. *Citizen Science: Theory and Practice*, *11*(1), 1–15. https://doi.org/10.5334/cstp.868

Greenwood, S., Chen, J. C., Chen, C. T., & Jump, A. S. (2014). Strong topographic sheltering effects lead to spatially complex treeline advance and increased forest density in a subtropical mountain

region. *Global Change Biology*, *20*(12), 3756–3766. https://doi.org/10.1111/gcb.12710

Greig, E. I., Wood, E. M., & Bonter, D. N. (2017). Winter range expansion of a hummingbird is associated with urbanization and supplementary feeding. *Proceedings of the Royal Society B: Biological Sciences*, *284*(1852). https://doi.org/10.1098/rspb.2017.0256

Guillera-Arroita, G., Lahoz-Monfort, J. J., Elith, J., Gordon, A., Kujala, H., Lentini, P. E., Mccarthy, M. A., Tingley, R., & Wintle, B. A. (2015). Is my species distribution model fit for purpose? Matching data and models to applications. *Global Ecology and Biogeography*, *24*(3), 276–292. https://doi.org/10.1111/geb.12268

Harris, J. B. C., Dwi Putra, D., Gregory, S. D., Brook, B. W., Prawiradilaga, D. M., Sodhi, N. S., Wei, D., & Fordham, D. A. (2014). Rapid deforestation threatens mid-elevational endemic birds but climate change is most important at higher elevations. *Diversity and Distributions*, *20*(7), 773–785. https://doi.org/10.1111/ddi.12180

Harris, J. B. C., Şekercioğlu, Ç. H., Sodhi, N. S., Fordham, D. A., Paton, D. C., & Brook, B. W. (2011). The tropical frontier in avian climate impact research. *Ibis*, *153*(4), 877–882. https://doi.org/10.1111/j.1474-919X.2011.01166.x

Horns, J. J., Adler, F. R., & Şekercioğlu, Ç. H. (2018). Using opportunistic citizen science data to estimate avian population trends. *Biological Conservation*, *221*, 151–159. https://doi.org/10.1016/j.biocon.2018.02.027

Jenouvrier, S. (2013). Impacts of climate change on avian populations. *Global Change Biology*, *19*(7), 2036–2057. https://doi.org/10.1111/gcb.12195

Johnson, P. C. D., Barry, S. J. E., Ferguson, H. M., & Pie, M. (2015). *Power analysis for generalized linear mixed models in ecology and evolution*. 133–142. https://doi.org/10.1111/2041-210X.12306

Johnston, A., Hochachka, W. M., Strimas-Mackey, M. E., Ruiz Gutierrez, V., Robinson, O. J., Miller, E. T., Auer, T., Kelling, S. T., & Fink, D. (2021). Analytical guidelines to increase the value of community science data: An example using eBird data to estimate species distributions. *Diversity and Distributions*, *27*(7), 1265–1277. https://doi.org/10.1111/DDI.13271

Kelling, S., Johnston, A., Bonn, A., Fink, D., Ruiz-Gutierrez, V., Bonney, R., Fernandez, M., Hochachka, W. M., Julliard, R., Kraemer, R., & Guralnick, R. (2019). Using Semistructured Surveys to Improve Citizen Science Data for Monitoring Biodiversity. *BioScience*, *69*(3), 170–179. https://doi.org/10.1093/biosci/biz010

Kelling, S., Johnston, A., Hochachka, W. M., Iliff, M., Fink, D., Gerbracht, J., Lagoze, C., La Sorte, F. A., Moore, T., Wiggins, A., Wong, W. K., Wood, C., & Yu, J. (2015). Can observation skills of citizen scientists be estimated using species accumulation curves? *PLoS ONE*, *10*(10), 1–20. https://doi.org/10.1371/journal.pone.0139600

Kuo, C. C., Liu, Y. C., Su, Y., Liu, H. Y., & Lin, C. T. (2022). *Responses of alpine summit vegetation under climate change in the transition zone between subtropical and tropical humid environment*. 1–13. https://doi.org/10.1038/s41598-022-17682-2

Lawler, J. J., Ackerly, D. D., Albano, C. M., Anderson, M. G., Dobrowski, S. Z., Gill, J. L., Heller, N. E., Pressey, R. L., Sanderson, E. W., & Weiss, S. B. (2015). *The theory behind , and the challenges of , conserving nature ' s stage in a time of rapid change*. *29*(3), 618–629. https://doi.org/10.1111/cobi.12505

Lawlor, J. A., Comte, L., Grenouillet, G., Lenoir, J., Baecher, J. A., Bandara, R. M. W. J., Bertrand, R., Chen, I. C., Diamond, S. E., Lancaster, L. T., Moore, N., Murienne, J., Oliveira, B. F., Pecl, G. T., Pinsky, M. L., Rolland, J., Rubenstein, M., Scheffers, B. R., Thompson, L. M., … Sunday, J. (2024). Mechanisms, detection and impacts of species redistributions under climate change. In *Nature Reviews Earth*

and Environment (Vol. 5, Issue 5, pp. 351–368). https://doi.org/10.1038/s43017-024-00527-z

Lenoir, J., Bertrand, R., Comte, L., Bourgeaud, L., Hattab, T., Murienne, J., & Grenouillet, G. (2020). Species better track climate warming in the oceans than on land. *Nature Ecology and Evolution*, *4*(8), 1044–1059. https://doi.org/10.1038/s41559-020-1198-2

Lin, W.-L., Ding, T.-S., Juan, C.-S., Lin, R.-S., Pan, C.-Y., Wu, J.-L., & Yang, Y.-H. (2026). *The 2026 TWBF Checklist of the Birds of Taiwan*. Taiwan Wild Bird Federation.

Linck, E. B. (2025). *What Is an Elevational Range ? 206*(4).

Liu, C., Newell, G., & White, M. (2019). *The effect of sample size on the accuracy of species distribution models: considering both presences and pseudo-absences or background sites*. *42*, 535–548. https://doi.org/10.1111/ecog.03188

Louthan, A. M., Doak, D. F., & Angert, A. L. (2015). Where and when do species interactions set range limits? *Trends in Ecology and Evolution*, *30*(12), 780–792. https://doi.org/10.1016/j.tree.2015.09.011

Marjakangas, E.-L., Bosco, L., Versluijs, M., Xu, Y., Santangeli, A., Holopainen, S., Mäkeläinen, S., Herrando, S., Keller, V., Voříšek, P., Brotons, L., Johnston, A., Princé, K., Willis, S. G., Aghababyan, K., Ajder, V., Balmer, D. E., Bino, T., Ali Boyla, K., … Lehikoinen, A. (2023). Ecological barriers mediate spatiotemporal shifts of bird communities at a continental scale. *Proceedings of the National Academy of Sciences*, *120*(23). https://doi.org/10.1073/PNAS.2213330120

Mason, B. M., Mesaglio, T., Barratt Heitmann, J., Chandler, M., Chowdhury, S., Gorta, S. B. Z., Grattarola, F., Groom, Q., Hitchcock, C., Hoskins, L., Lowe, S. K., Marquis, M., Pernat, N., Shirey, V., Baasanmunkh, S., & Callaghan, C. T. (2025). iNaturalist accelerates biodiversity research. *BioScience*, *75*(11), 953–965. https://doi.org/10.1093/biosci/biaf104

Matysioková, B., & Remeš, V. (2022). Stronger negative species interactions in the tropics supported by a global analysis of nest predation in songbirds. *Journal of Biogeography*, *49*(3), 511–522. https://doi.org/10.1111/jbi.14321

McCain, C., Szewczyk, T., & Bracy Knight, K. (2016). Population variability complicates the accurate detection of climate change responses. *Global Change Biology*, *22*(6), 2081–2093. https://doi.org/10.1111/GCB.13211

Morueta-Holmea, N., Engemann, K., Sandoval-Acuña, P., Jonas, J. D., Segnitz, R. M., & Svenning, J.-C. (2015). Strong upslope shifts in Chimborazo's vegetation over two centuries since Humboldt. *Proceedings of the National Academy of Science*, *112*(41), 12741–12745. https://doi.org/10.1073/pnas.1509938112

Namkhan, M., Gale, G. A., Savini, T., & Tantipisanuh, N. (2021). Loss and vulnerability of lowland forests in mainland Southeast Asia. *Conservation Biology*, *35*(1), 206–215. https://doi.org/10.1111/cobi.13538

Neate-Clegg, M. H. C., Horns, J. J., Adler, F. R., Kemahlı Aytekin, M. Ç., & Şekercioğlu, Ç. H. (2020). Monitoring the world's bird populations with community science data. *Biological Conservation*, *248*, 108653. https://doi.org/10.1016/j.biocon.2020.108653

Neate-Clegg, M. H. C., Jones, S. E. I., Burdekin, O., Jocque, M., & Şekercioğlu, Ç. H. (2018). Elevational changes in the avian community of a Mesoamerican cloud forest park. *Biotropica*, *50*(5), 805–815. https://doi.org/10.1111/btp.12596

Neate-Clegg, M. H. C., Jones, S. E. I., Tobias, J. A., Newmark, W. D., & Şekercioğlu, Ç. H. (2021). Ecological correlates of elevational range shifts in tropical birds. *Frontiers in Ecology and Evolution*, *9*, 621749. https://doi.org/10.3389/fevo.2021.621749

Neate-Clegg, M. H. C., O'Brien, T. G., Mulindahabi, F., & Şekercioğlu, Ç. H. (2020). A disconnect between upslope shifts and climate change in an Afrotropical bird community. *Conservation Science and Practice*, *2*(11), e291. https://doi.org/10.1111/csp2.291

Neate-Clegg, M. H. C., & Tingley, M. W. (2023). Building a mechanistic understanding of climate-driven elevational shifts in birds. *PLoS Climate*, *2*(3), e0000174. https://doi.org/10.1371/journal.pclm.0000174

Neate-Clegg, M. H. C., Tonelli, B. A., & Tingley, M. W. (2024). Advances in breeding phenology outpace latitudinal and elevational shifts for North American birds tracking temperature. *Nature Ecology & Evolution*, *8*, 2027–2036. https://doi.org/10.1038/s41559-024-02536-z

Neate-Clegg, M. H. C., Tonelli, B. A., Youngflesh, C., Wu, J. X., Montgomery, G. A., & Tingley, M. W. (2023). Traits shaping urban tolerance in birds differ around the world. *Current Biology*, *33*(9), 1677-1688.e6. https://doi.org/10.1016/j.cub.2023.03.024

NSTC, & MOENV. (2024). *Climate Change in Taiwan: National Scientific Report 2024*.

Ocampo-Peñuela, N., de Alfaro, S., Neate-Clegg, M. H. C., de Alfaro, L., Bjegovic, K., & Winton, R. S. (2025). Human development, societal stability and bird capital predict global tourist eBirding activity. *People and Nature*, *7*(10), 2486–2499. https://doi.org/10.1002/pan3.70105

Ocampo-Peñuela, N., & Pimm, S. L. (2015). Elevational ranges of montane birds and deforestation in the Western Andes of Colombia. *PLoS ONE*, *10*(12). https://doi.org/10.1371/journal.pone.0143311

Paquette, A., & Hargreaves, A. L. (2021). Biotic interactions are more often important at species' warm versus cool range edges. In *Ecology Letters* (Vol. 24, Issue 11, pp. 2427–2438). https://doi.org/10.1111/ele.13864

Parmesan, C., & Yohe, G. (2003). A globally coherent fingerprint of climate change impacts across

natural systems. *Nature*, *421*(6918), 37–42. https://doi.org/10.1038/nature01286

Paxton, E. H., Camp, R. J., Gorresen, P. M., Crampton, L. H., Jr, D. L. L., & Vanderwerf, E. A. (2016). Collapsing avian community on a Hawaiian island. *Science Advances*, *2*(9), 1–8. https://doi.org/10.1126/sciadv.1600029

Pedersen, E. J., Miller, D. L., Simpson, G. L., & Ross, N. (2019). Hierarchical generalized additive models in ecology : an introduction with mgcv. *PeerJ*, *7*, e6876. https://doi.org/10.7717/peerj.6876

Phillips, S. J., Dudík, M., Elith, J., Graham, C. H., Lehmann, A., Leathwick, J., & Ferrier, S. (2009). Sample selection bias and presence-only distribution models: Implications for background and pseudo-absence data. *Ecological Applications*, *19*(1), 181–197. https://doi.org/10.1890/07-2153.1;PAGEGROUP:STRING:PUBLICATION

Rubenstein, M. A., Weiskopf, S. R., Bertrand, R., Carter, S. L., Comte, L., Eaton, M. J., Johnson, C. G., Lenoir, J., Lynch, A. J., Miller, B. W., Morelli, T. L., Rodriguez, M. A., Terando, A., & Thompson, L. M. (2023). Climate change and the global redistribution of biodiversity: substantial variation in empirical support for expected range shifts. *Environmental Evidence*, *12*(1), 1–21. https://doi.org/10.1186/s13750-023-00296-0

Rumpf, S. B., Hülber, K., Zimmermann, N. E., & Dullinger, S. (2019). Elevational rear edges shifted at least as much as leading edges over the last century. *Global Ecology and Biogeography*, *28*(4), 533–543. https://doi.org/10.1111/geb.12865

Şekercioğlu, Ç. H., Schneider, S. H., Fay, J. P., & Loarie, S. R. (2008). Climate change, elevational range shifts, and bird extinctions. *Conservation Biology*, *22*(1), 140–150. https://doi.org/10.1111/j.1523-1739.2007.00852.x

Somveille, M., Freeman, B. G., La Sorte, F. A., & Tuanmu, M. N. (2026). Climate, ecological dynamics, and

the seasonal distribution of birds in mountains. *Science Advances*, *12*(6), eadz5547. https://doi.org/10.1126/sciadv.adz5547

Sullivan, B. L., Wood, C. L., Iliff, R. E., Bonney, D. F., & Kelling, S. (2009). eBird: a citizen-based bird observation network in the biological sciences. *Biological Conservation*, *142*, 2282–2292.

Szabo, J. K., Vesk, P. A., Baxter, P. W. J., & Possingham, H. P. (2010). Regional avian species declines estimated from volunteer-collected long-term data using List Length Analysis. *Ecological Applications*, *20*(8), 2157–2169. https://doi.org/10.1890/09-0877.1

Theobald, E. J., Ettinger, A. K., Burgess, H. K., DeBey, L. B., Schmidt, N. R., Froehlich, H. E., Wagner, C., HilleRisLambers, J., Tewksbury, J., Harsch, M. A., & Parrish, J. K. (2015). Global change and local solutions: Tapping the unrealized potential of citizen science for biodiversity research. *Biological Conservation*, *181*, 236–244. https://doi.org/10.1016/j.biocon.2014.10.021

Tingley, M. W., Koo, M. S., Moritz, C., Rush, A. C., & Beissinger, S. R. (2012). The push and pull of climate change causes heterogeneous shifts in avian elevational ranges. *Global Change Biology*, *18*(11), 3279–3290. https://doi.org/10.1111/j.1365-2486.2012.02784.x

Tingley, M. W., Monahan, W. B., Beissinger, S. R., & Moritz, C. (2009). Birds track their Grinnellian niche through a century of climate change. *Proceedings of the National Academy of Science*, *106*(SUPPL. 2), 19637–19643. https://doi.org/10.1073/pnas.0901562106

Tobias, J. A., Sheard, C., Pigot, A. L., Devenish, A. J. M., Yang, J., Neate-Clegg, M. H. C., Alioravainen, N., Weeks, T. L., Barber, R. A., Walkden, P. A., MacGregor, H. E. A., Jones, S. E. I., Vincent, C., Phillips, A. G., Marples, N. M., Montaño-Centellas, F., Leandro-Silva, V., Claramunt, S., Darski, B., … Schleunning, M. (2022). AVONET: morphological, ecological and geographical data for all birds. *Ecology Letters*, *25*(3), 581–597. https://doi.org/10.1111/ele.13898

Tsai, P.-Y., Ko, C.-J., Chia, S. Y., Lu, Y.-J., & Tuanmu, M.-N. (2021). New insights into the patterns and drivers of avian altitudinal migration from a growing crowdsourcing data source. *Ecography*, *44*(1), 75–86. https://doi.org/10.1111/ecog.05196

Tsai, P.-Y., & Tuanmu, M.-N. (2024). *Spatiotemporal and Environmental Completeness of eBird Data in Taiwan*. 8–11. https://doi.org/10.3897/biss.8.134514

Walker, J., & Taylor, P. D. (2017). *Using eBird data to model population change of migratory bird species*. *12*(1).

White, E. R. (2019). Minimum Time Required to Detect Population Trends: The Need for Long-Term Monitoring Programs. *BioScience*, *69*(1), 26–39. https://doi.org/10.1093/biosci/biy144

Wu, T.-Y., Lee, P.-F., Lin, R.-S., Wu, J.-L., & Walther, B. A. (2012). Modeling the distribution of rare or cryptic bird species of Taiwan. *Taiwania*, *57*(4), 342–358.

Youngflesh, C., Socolar, J., Amaral, B. R., Arab, A., Guralnick, R. P., Hurlbert, A. H., LaFrance, R., Mayor, S. J., Miller, D. A. W., & Tingley, M. W. (2021). Migratory strategy drives species-level variation in bird sensitivity to vegetation green-up. *Nature Ecology and Evolution*. https://doi.org/10.1038/s41559-021-01442-y

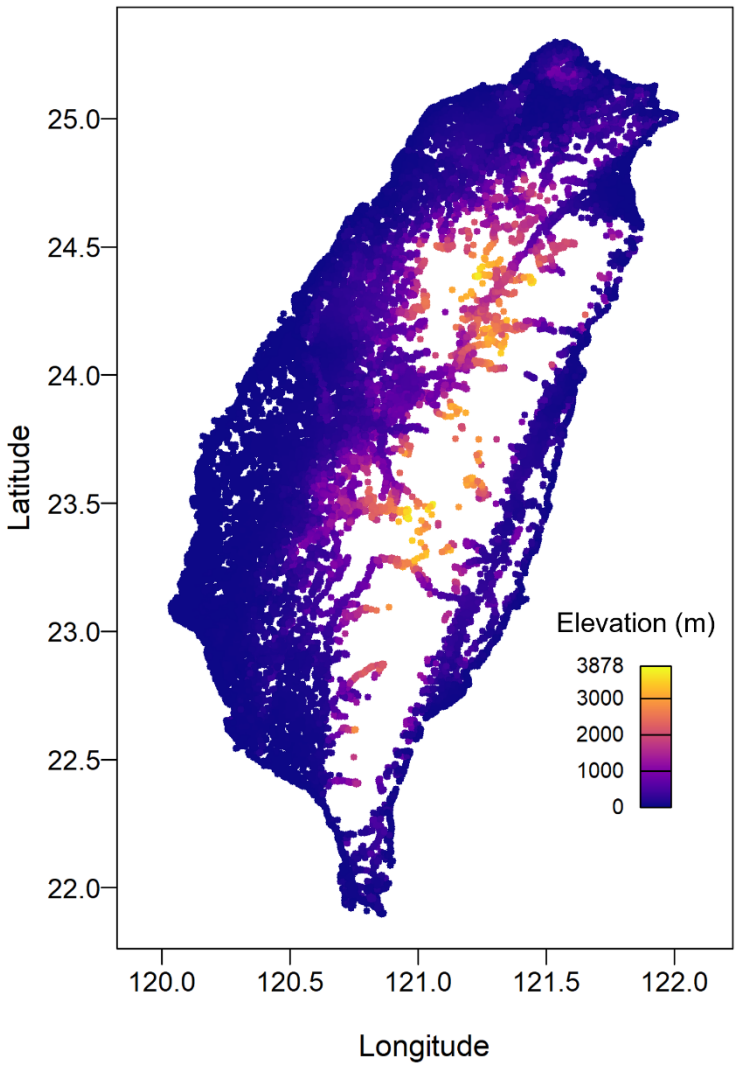

Figure 1. Map of Taiwan showing the location of eBird checklist localities. Localities are colored by elevation from sea level (dark purple) to the highest checklist at 3878 m (yellow).

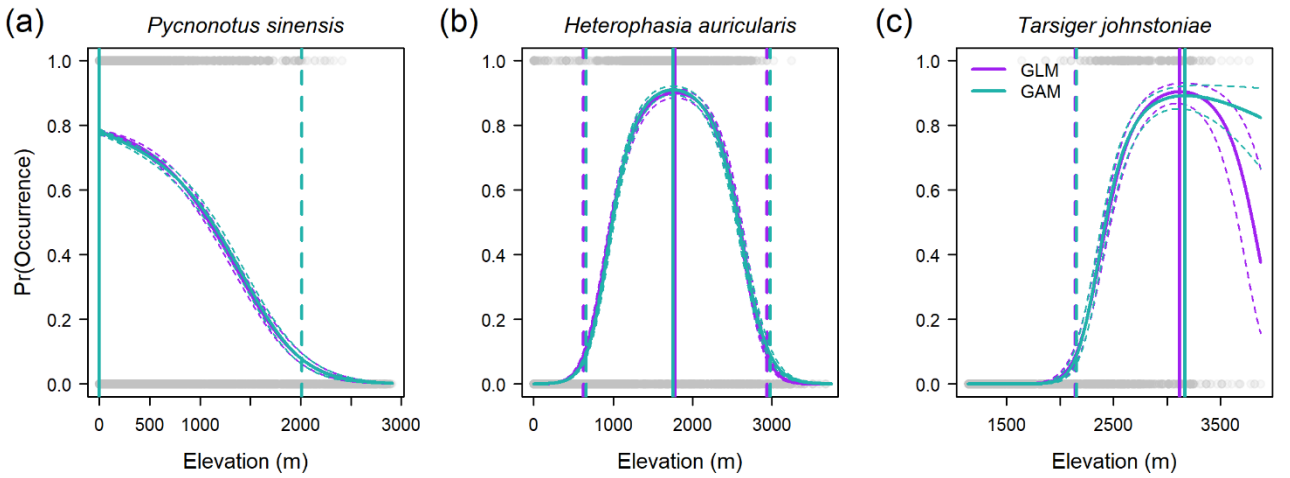

Figure 2. Occurrence probability curves across elevation for three bird species in Taiwan. The three common species provide examples of a lowland species (a, *Pycnonotus sinensis*), a mid-elevation species (b, *Heterophasia auricularis*), and a mountaintop species (c, *Tarsiger johnstoniae*). For each species, occurrence probability was modeled as a function of elevation in either a generalized linear model (GLM) with quadratic effect of elevation, or in a generalized additive model (GAM) with a smoothing effect of elevation (k = 3). Points show presence/absences and the curves represent the predicted probability of occurrence. Unbroken vertical lines indicate the estimated peak elevation while dashed lines indicate the lower and upper range limit i.e., where the probability of occurrence reaches 10% of the maximum.

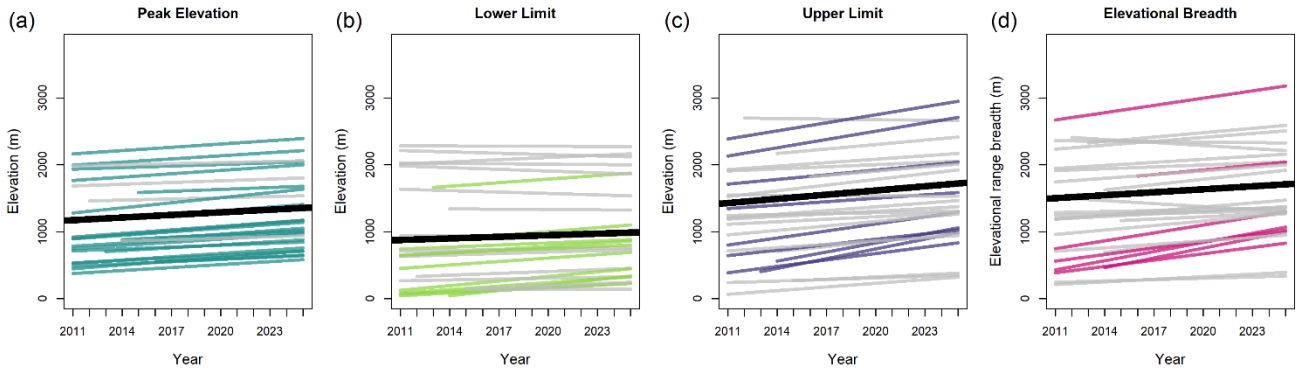

Figure 3. Elevational range shifts across 69 species of resident land birds in Taiwan. Thick black lines represent mean trends over time in (a) peak elevations, (b) lower limits, (c) upper limits, and (d) elevational range. Thin lines represent species-specific trends and are gray when the Bayesian credible interval on the slope estimate overlaps 0. The length of each line is determined by the number of years of estimates available for a given species.

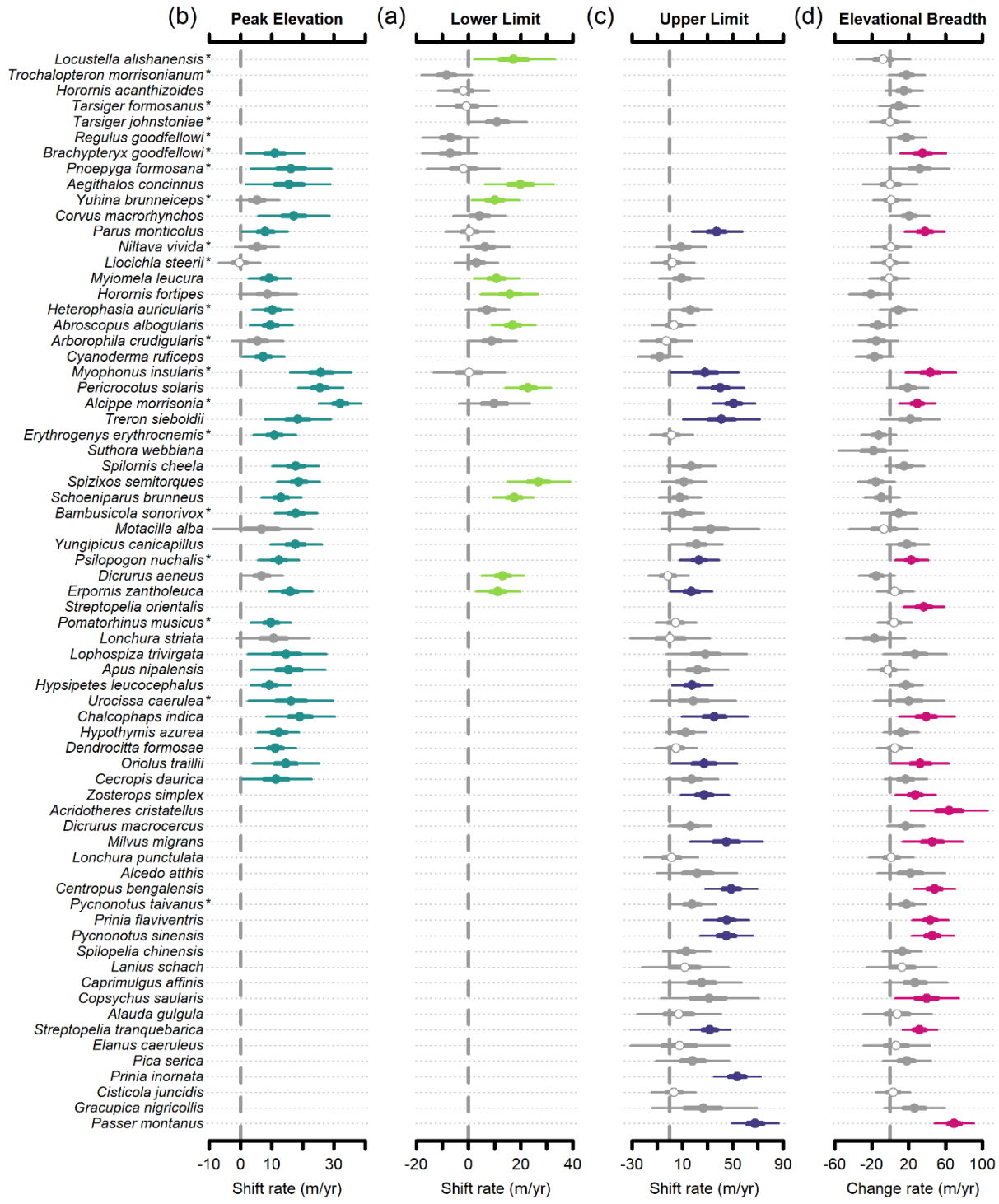

Figure 4. Elevational shift rates across 69 species of resident land birds in Taiwan. Points represent species-specific trends over time in (a) peak elevation, (b) lower limit, (c) upper limit, and (d) elevational breadth. Thin lines represent 95% credible intervals and are gray when they overlap 0. Thick lines represent the interquartile range of the posteriors, with points having a white center when the interquartile range overlaps 0. Asterisks denote endemic species.

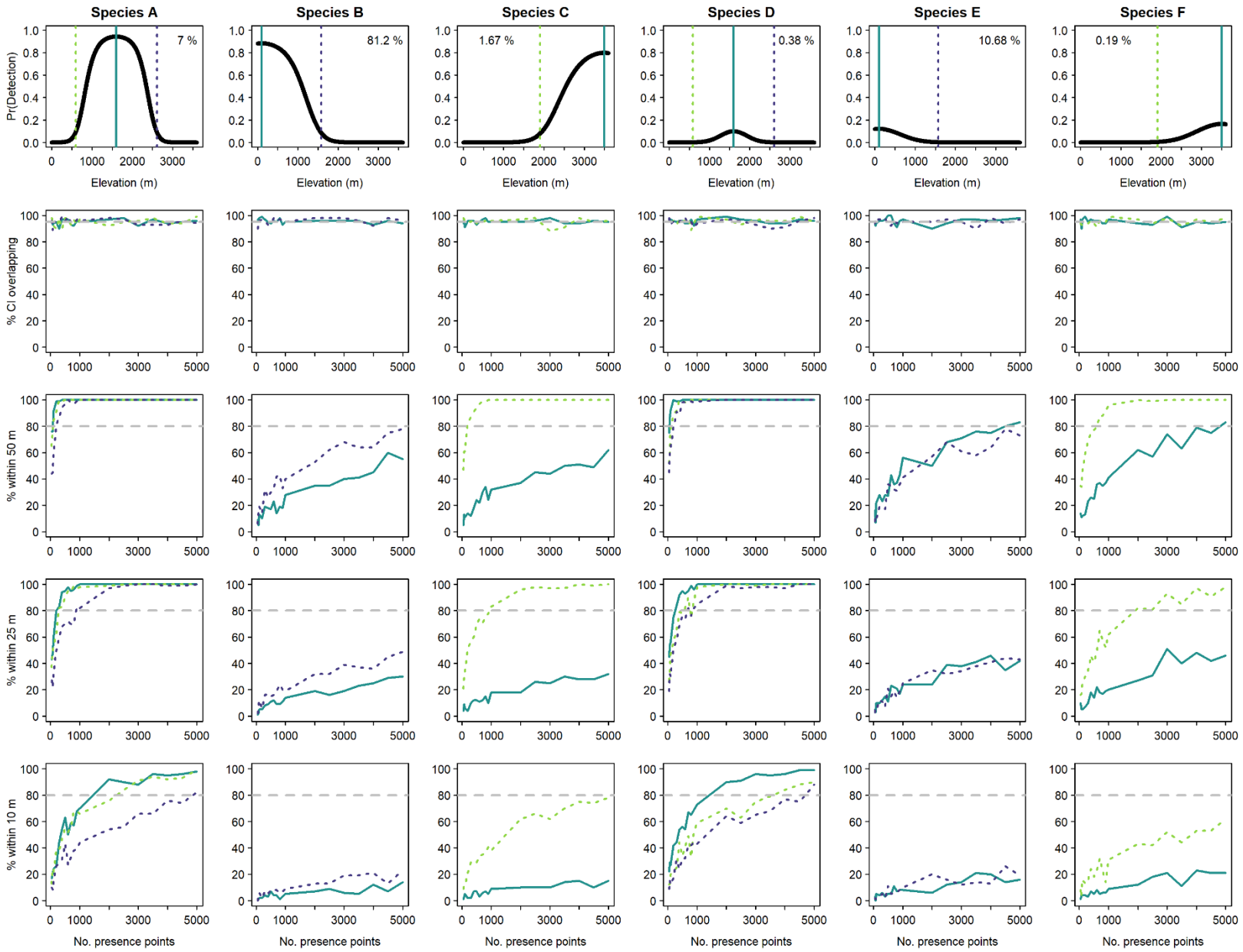
Species A
Species B
Species C
Species D
Species E
Species F
7 %
81.2 %
1.67 %
0.38 %
10.68 %
0.19 %
Pr(Detection)
% CI overlapping
% within 50 m
% within 25 m
% within 10 m
Elevation (m)
No. presence points

Figure 5. Results from power analyses to determine the number of presence points needed to estimate elevational metrics for six hypothetical species. Each hypothetical species (top row) had a pre-defined curve of occurrence probability (top row) with known peak elevation (solid vertical line) and lower and upper range limits (dotted lines). Species A–C are common species with mid-elevation, lowland, and highland distributions, respectively; species D–F have similar distributions to species A–C but are scarce (i.e., recorded less frequently). Percentages indicate the mean percentage of checklists on which the species was present. For each species, presence/absences were simulated based on the occurrence probability curves and filtered down to a defined number of presence points, *n*. Quadratic GLMs were then fit to these presence/absences, deriving estimates of elevation and range limits. These metric estimates were then compared to the "true" known metrics. The second row shows the percentage of simulations for which the 95% confidence interval of the estimate overlapped the truth. Here, the horizontal dashed line indicates when 95% of simulations resulted in coverage. Rows three through five show the percentage of simulations resulting in estimates that were within 50 m, 25 m, or 10 m of the truth. For these rows, the horizontal dashed line indicates when 80% of simulations (the typical threshold for power analyses) resulted in suitable accuracy.

Supporting Information

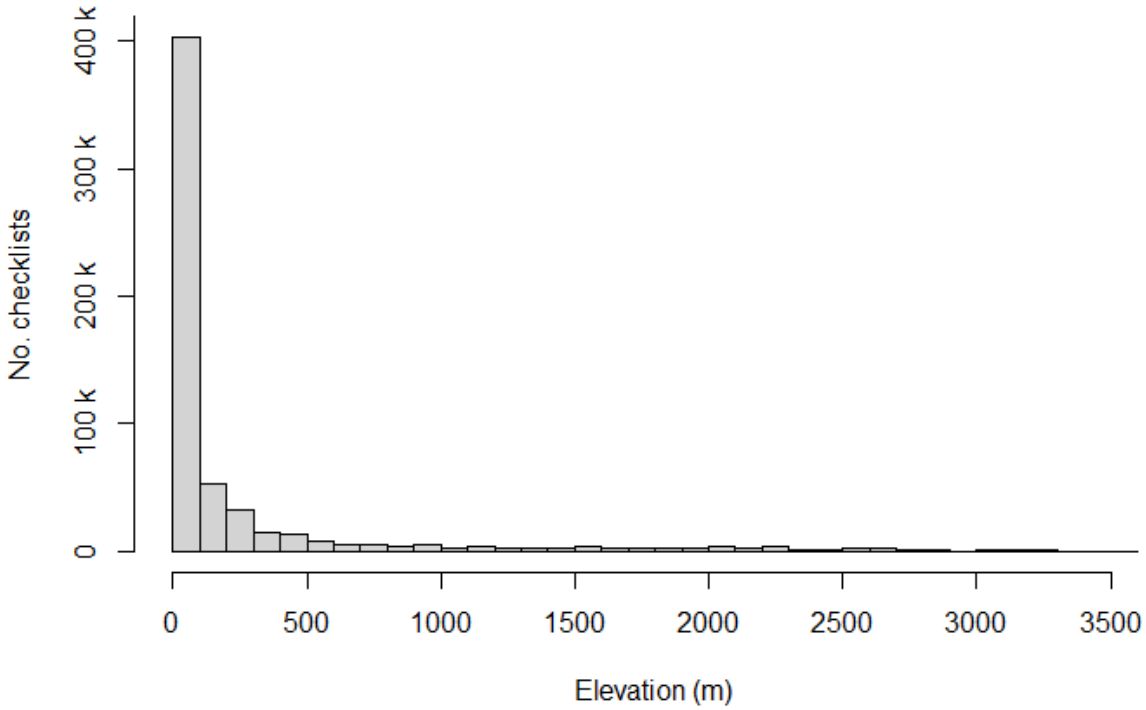

Figure S1. Histogram of the elevational distribution of 593,410 eBird checklists across Taiwan from 2011 to 2025.

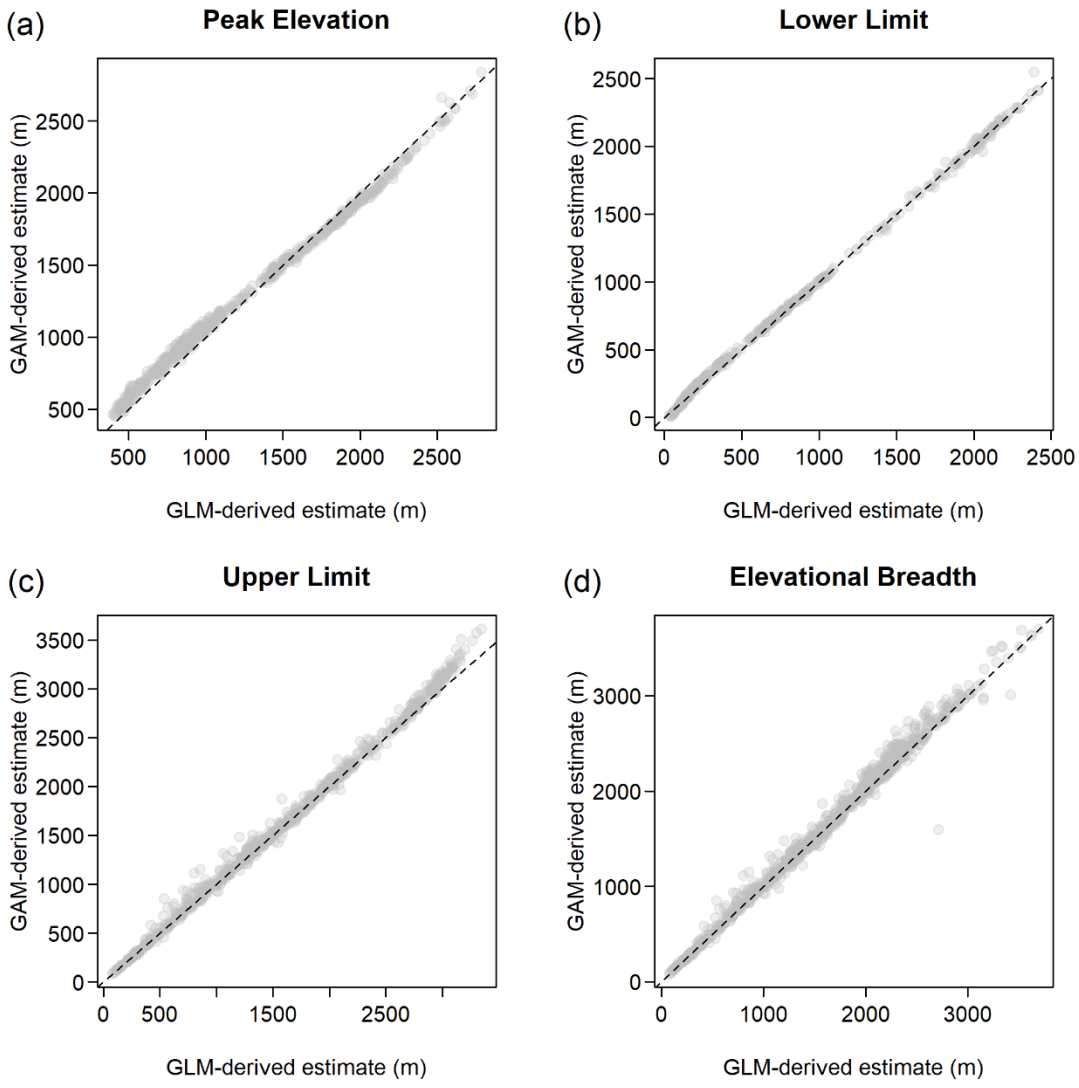

Figure S2. Correlation between GAM-derived and GLM-derived estimates of elevational metrics for 69 bird species in Taiwan. Each point represents the estimate of an elevational metric for a particular species and year. Occurrence probability across elevation was modeled in either a generalized additive model (GAM) as a smooth function of elevation, or in a generalized linear model (GLM) as a quadratic function of elevation. From these occurrence curves, the peak elevation (a) is the elevation of the highest occurrence probability, the lower (b) and upper limits (c) are the elevations at which occurrence probability was 10% of the maximum, and the elevational breadth (d) is the difference in elevation between the upper and lower limit. Where range limits were not estimated for a species (due to being at sea level or the highest elevation), the topographic boundary was used to calculate elevational range instead. Points have 25% transparency. The dashed line indicates 1:1 correspondence.

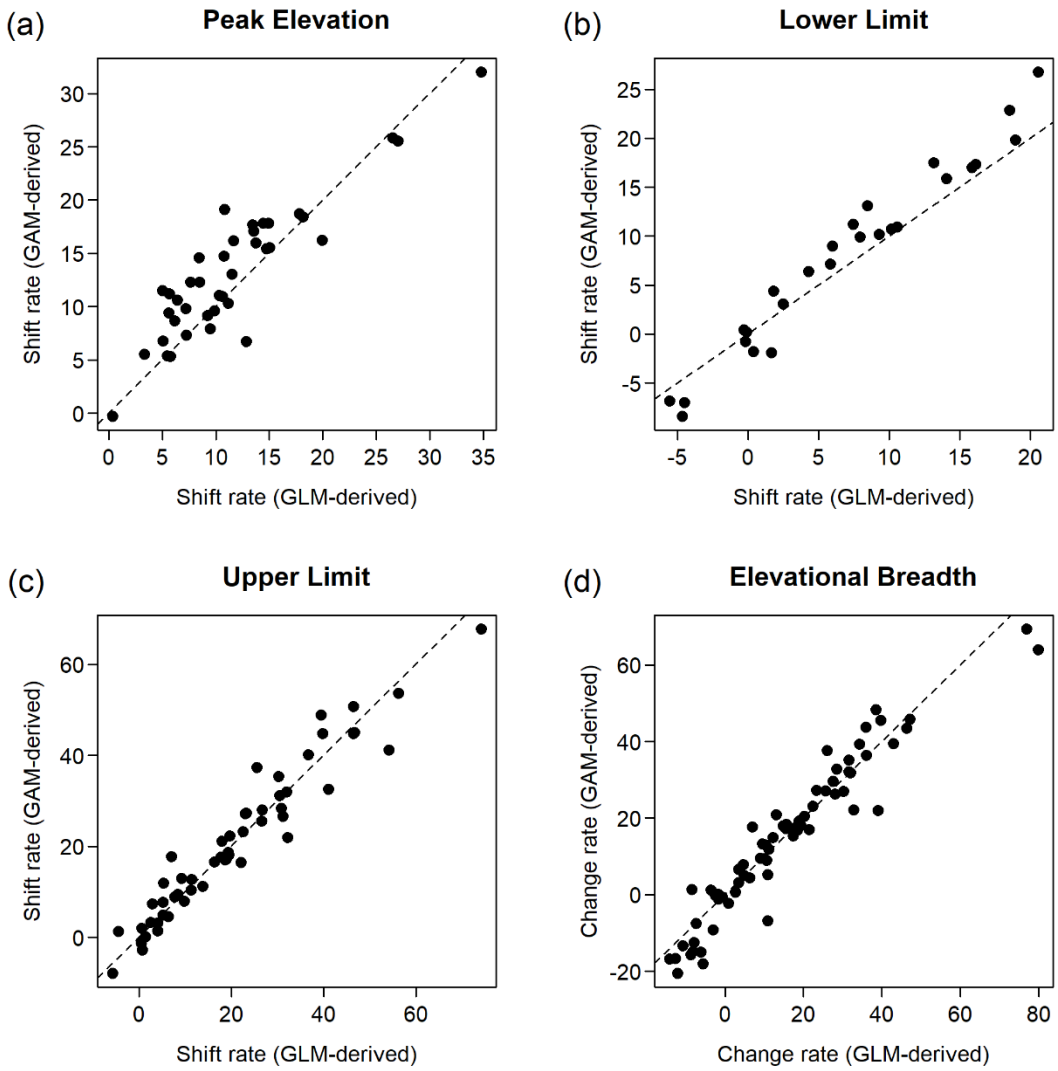

Figure S3. Correlation between GAM-derived and GLM-derived species-specific estimates of elevational shift rates for 69 bird species in Taiwan. Each point represents the estimated shift/change rate for a particular species for four elevational metrics: (a) peak elevation, (b) lower limit, (c) upper limit, and (d) elevational breadth. These four metrics were derived from either a generalized additive model (GAM) with a smooth function of elevation, or a generalized linear model (GLM) with a quadratic function of elevation. The peak elevation (a) is the elevation of the highest occurrence probability, the lower (b) and upper limits (c) are the elevations at which occurrence probability was 10% of the maximum, and the elevational breadth (d) is the difference in elevation between the upper and lower limit. Where range limits were not estimated for a species (due to being at sea level or the highest elevation), the topographic boundary was used to calculate elevational range instead. The dashed line indicates 1:1 correspondence.

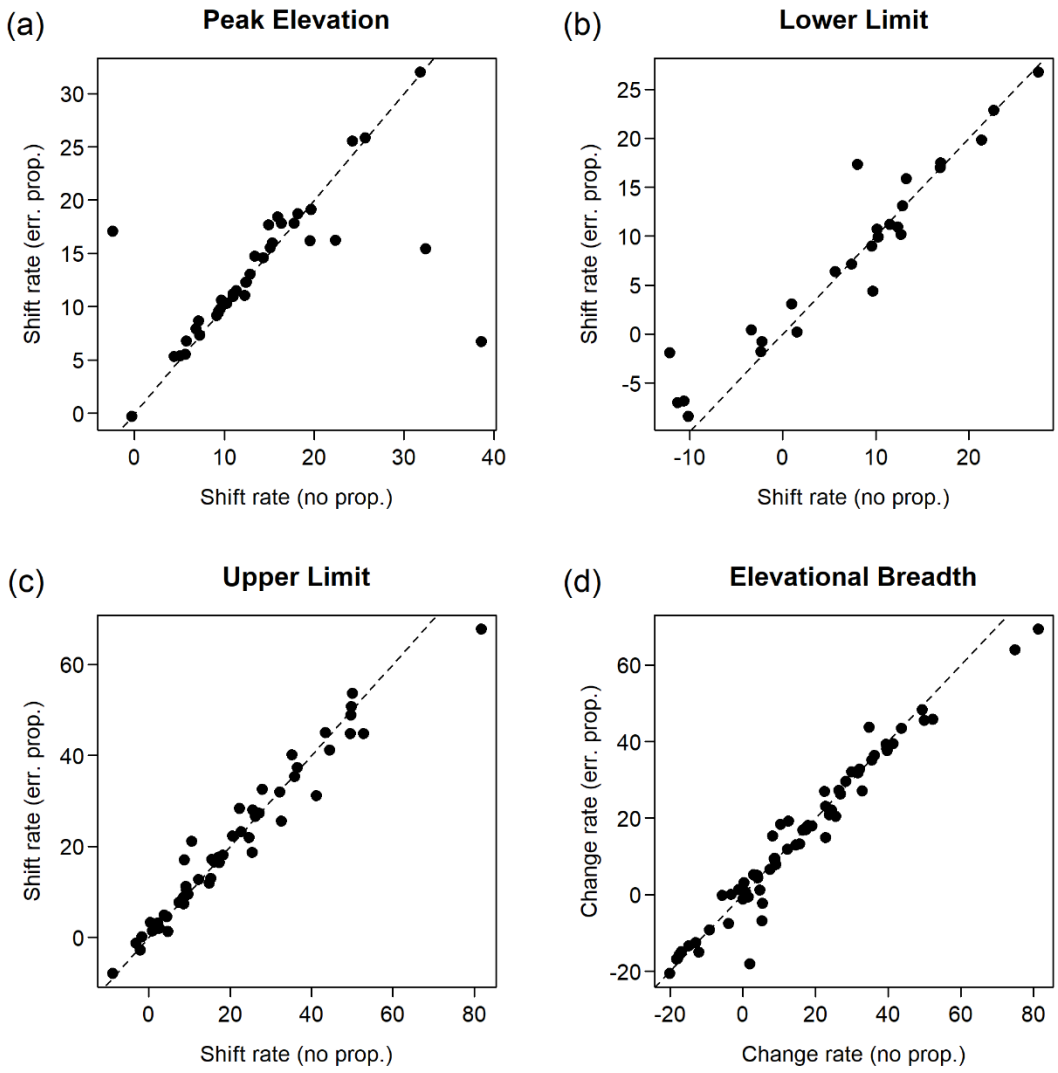

Figure S4. Correlation between GAM-derived species-specific estimates of elevational shift rates with and without error propagation for 69 bird species in Taiwan. Each point represents the estimated shift/change rate for a particular species for four elevational metrics: (a) peak elevation, (b) lower limit, (c) upper limit, and (d) elevational breadth. These four metrics were derived from either a generalized additive model (GAM) where uncertainty in the metric estimate was incorporated into the model, from a GAM where uncertainty was not incorporated. The peak elevation (a) is the elevation of the highest occurrence probability, the lower (b) and upper limits (c) are the elevations at which occurrence probability was 10% of the maximum, and the elevational breadth (d) is the difference in elevation between the upper and lower limit. Where range limits were not estimated for a species (due to being at sea level or the highest elevation), the topographic boundary was used to calculate elevational range instead. The dashed line indicates 1:1 correspondence.

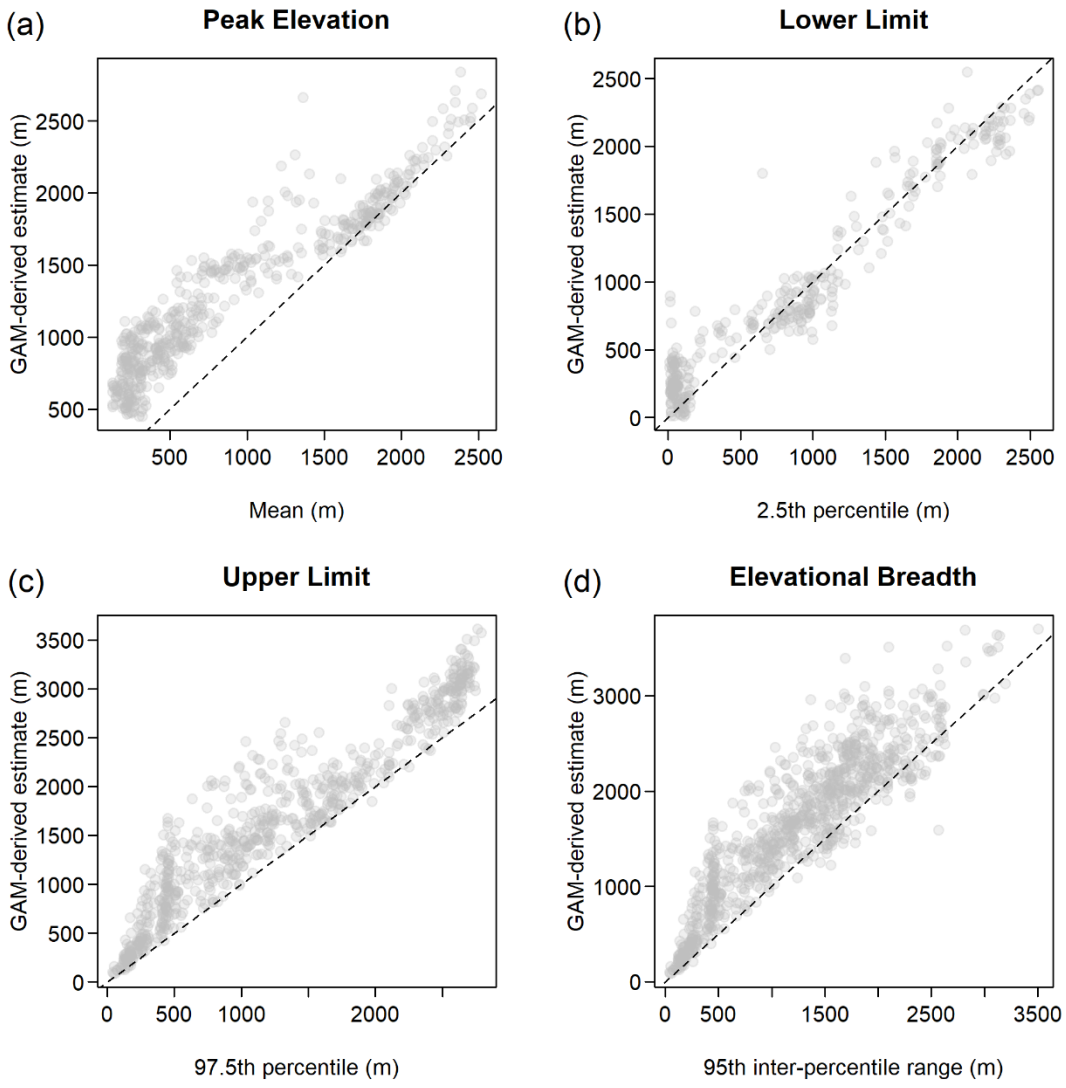

Figure S5. Correlation between GAM-derived and simple estimates of elevational metrics for 69 bird species in Taiwan. Each point represents the estimate of an elevational metric for a particular species and year. For the GAMs (generalized additive models), occurrence probability was modeled as a smooth function of elevation. From these occurrence curves, the peak elevation (a) is the elevation of the highest occurrence probability, the lower (b) and upper limits (c) are the elevations at which occurrence probability was 10% of the maximum, and the elevational range (d) is the difference in elevation between the upper and lower limit. These estimates are compared to simple metrics based on the elevations of all presences: the mean (a), the 2.5th percentile (b), the 97.5th percentile (c), and the 95th inter-percentile range. Where range limits were not estimated for a species (due to being at sea level or the highest elevation), the topographic boundary was used to calculate elevational range instead. Points have 25% transparency. The dashed line indicates 1:1 correspondence.

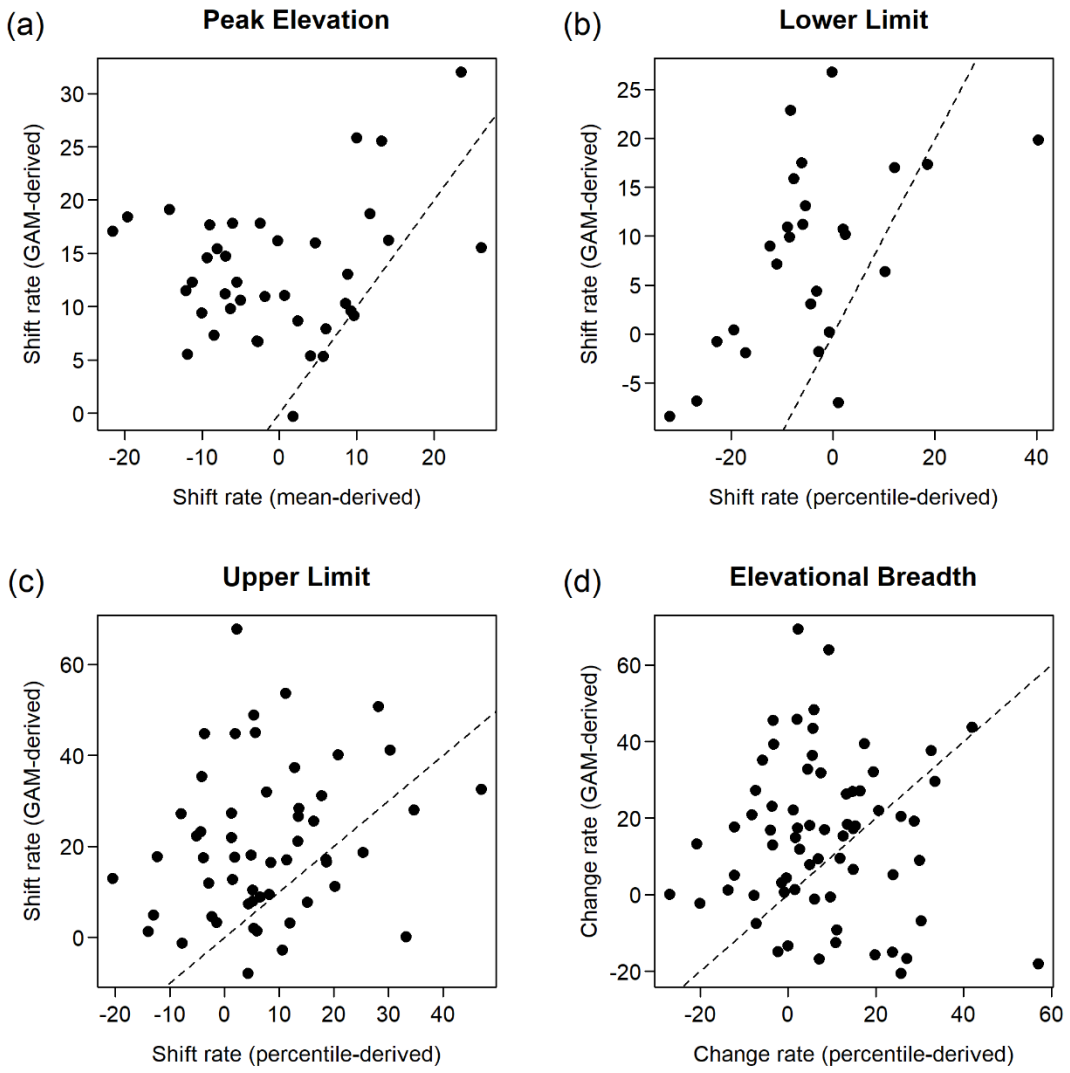

Figure S6. Correlation between GAM-derived and simply derived estimates of elevational shift rates with and without error propagation for 69 bird species in Taiwan. Each point represents the estimated shift/change rate for a particular species for four elevational metrics. For the GAMs (generalized additive models), occurrence probability was modeled as a smooth function of elevation. From these occurrence curves, the peak elevation (a) is the elevation of the highest occurrence probability, the lower (b) and upper limits (c) are the elevations at which occurrence probability was 10% of the maximum, and the elevational breadth (d) is the difference in elevation between the upper and lower limit. Shift rates from these estimates are compared to shift rates based on simple metrics calculated from the elevations of all presences: the mean (a), the 2.5th percentile (b), the 97.5th percentile (c), and the 95th inter-percentile range. Where range limits were not estimated for a species (due to being at sea level or the highest elevation), the topographic boundary was used to calculate elevational range instead. The dashed line indicates 1:1 correspondence.